科学论文结果呈现

史凯斌

首都医科大学附属北京天坛医院

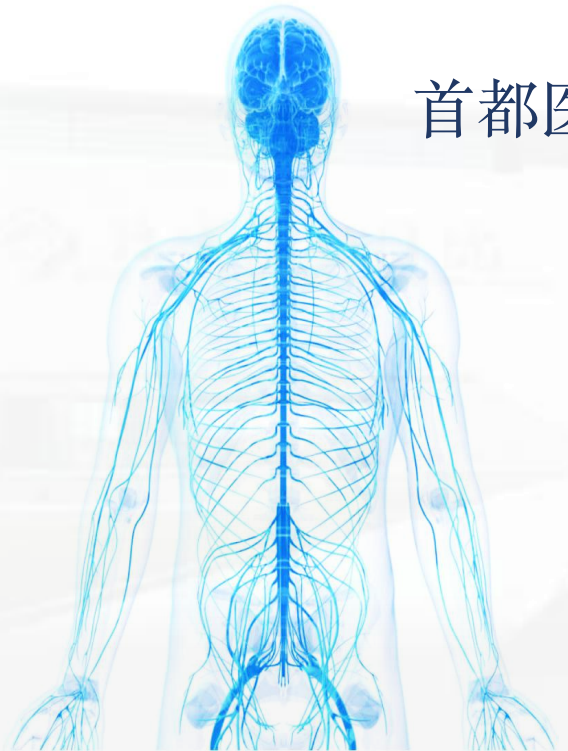

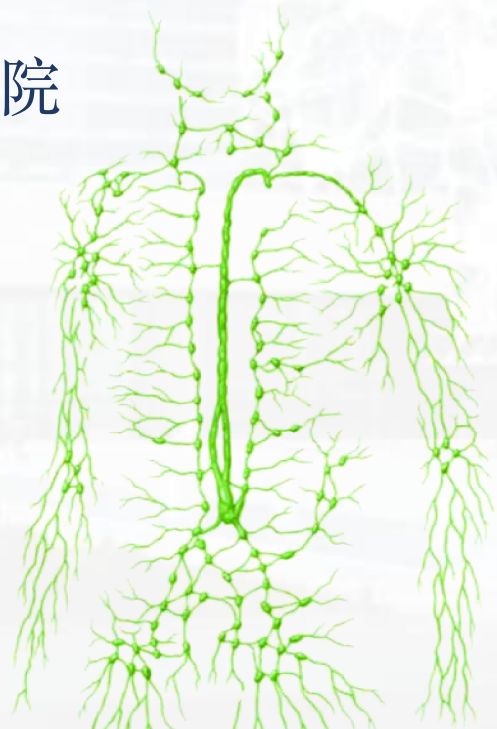

2022年2月

汇报提纲

一 为什么作图

二 作怎样的图

三 如何作好图

四 怎么注释图

一 为什么作图

應

殿試舉人臣劉春霖年三十歲直隸河間府肅寧縣人由拔貢生應光緒二十八年順天鄉試中式由舉人應光緒三十年會試中式恭應

殿試謹將三代胪色開具於後

臣對臣聞王者不咎改過故盛世有直言極諫之科學者義取匡時故貢士有盡忠竭愚之志昔漢文帝除誹謗之法而後賈山賈誼爭其致忠讜之謨武帝崇尚儒術詔舉賢良而後賈仲舒嚴安徐樂之徒羣集於闕下宋仁宗復制舉諸科除越職言事之禁而後蘇軾蘇轍對策極言時政闕失其於官治兵任之要裕財正俗之方類能指陳利其所以浮之自而杜之約者必本其所以約之由而從之皆扼要之論然臣謂理財於今日節流不如開源之尤要蓋自通商以來利源外溢雖百計節省而無救於貧開源之道在振興實業中國神皋沃壤幅員縱橫寒廓且地處溫帶之下百物皆宜則當講求農事人民四百兆善耐勞苦而且心思聰敏中外交通以後閱粵瀕海之人類能之造洋貨果其加意提倡不難日出新製則宜振興工藝歐西以商業之勝衰為國力之強弱輸帆交錯以爭海外利權中國商業不興漏卮日鉅抵制之道則宜擴充商欲圖務如此則野無曠土市無游民精華日呈然後利權可挽

皇上慎乃儉德而尤必廣開利源此不得不因時制宜者三也

曾祖永生 未仕故　祖昆 未仕故　父甦書 未仕故

ARTICLES

Mesenchymal and haematopoietic stem cells form a unique bone marrow niche

Simón Méndez-Ferrer[1,2]*, Tatyana V. Michurina[3], Francesca Ferraro[4], Amin R. Mazloom[5], Ben D. MacArthur[5]†, Sergio A. Lira[1], David T. Scadden[4], Avi Ma'ayan[5], Grigori N. Enikolopov[3] & Paul S. Frenette[1,2,6]

The cellular constituents forming the haematopoietic stem cell (HSC) niche in the bone marrow are unclear, with studies implicating osteoblasts, endothelial and perivascular cells. Here we demonstrate that mesenchymal stem cells (MSCs), identified using nestin expression, constitute an essential HSC niche component. Nestin$^+$ MSCs contain all the bone-marrow colony-forming-unit fibroblastic activity and can be propagated as non-adherent 'mesenspheres' that can self-renew and expand in serial transplantations. Nestin$^+$ MSCs are spatially associated with HSCs and adrenergic nerve fibres, and highly express HSC maintenance genes. These genes, and others triggering osteoblastic differentiation, are selectively downregulated during enforced HSC mobilization or β3 adrenoreceptor activation. Whereas parathormone administration doubles the number of bone marrow nestin$^+$ cells and favours their osteoblastic differentiation, *in vivo* nestin$^+$ cell depletion rapidly reduces HSC content in the bone marrow. Purified HSCs home near nestin$^+$ MSCs in the bone marrow of lethally irradiated mice, whereas *in vivo* nestin$^+$ cell depletion significantly reduces bone marrow homing of haematopoietic progenitors. These results uncover an unprecedented partnership between two distinct somatic stem-cell types and are indicative of a unique niche in the bone marrow made of heterotypic stem-cell pairs.

The identity of the cells forming the HSC niche remains unclear. Previous studies have shown that osteolineage cells control the niche size[1–3] and HSCs have been found preferentially localized in the endosteal region[2,4–10]. However, haematopoiesis can be sustained in extramedullary sites and selective osteoblast depletion[11,12] or expansion[13] does not acutely affect HSC numbers. HSCs have also been located preferentially in perivascular regions[14], near reticular cells that express high levels of the chemokine CXCL12 (also called SDF-1)[15]. However, the identity and function of these cells have not been clearly defined.

The movement of HSCs may provide an insight into their niche because it is directly regulated by the microenvironment. HSC mobilization requires signals from the sympathetic nervous system (SNS)[16,17], which under homeostasis lead to clock-controlled rhythmic oscillations of *Cxcl12* expression through the β_3-adrenergic receptor (β_3-AR, encoded by *Adrb3*)[18]. Sympathetic fibres in the bone marrow are associated with blood vessels and adventitial reticular cells connected by gap junctions, thereby forming a structural network called the neuro-reticular complex[19]. Here we have studied the stromal elements involved in this complex.

Nestin identifies rare SNS-innervated perivascular stromal cells

Through unrelated investigations, we have noted that bone marrow cells expressing the green fluorescent protein (GFP) under the regulatory elements of the nestin promoter[20] (hereafter referred to as *Nes*-GFP$^+$ cells) were relatively rare non-haematopoietic cells (4.0 ± 0.6% of the stromal CD45$^-$ population), representing a small subset of nucleated cells (0.08 ± 0.01% by fluorescence-activated cell sorting (FACS); 0.044 ± 0.001% by histology; Fig. 1a and Supplementary Fig. 1). *Nes*-GFP$^+$ cells also expressed the intermediate filament protein nestin (Fig. 1b and Supplementary Fig. 2) and were distinct from vascular endothelial cells because they did not express CD31 (also called PECAM) (Fig. 1c, d), CD34 or VE-cadherin (data not shown). However, they showed exclusively a perivascular distribution (Fig. 1d and Supplementary Fig. 3) in regions adjacent to the bone (Fig. 1e) or within the bone marrow parenchyma (Fig. 1f). Catecholaminergic nerve fibres were closely associated with *Nes*-GFP$^+$ cells (Fig. 1e, f, red staining; Supplementary Fig. 4). Furthermore, *Adrb3* expression was highly enriched in CD45$^-$ *Nes*-GFP$^+$ cells (Fig. 1g). *Cxcl12* expression was >50-fold higher in *Nes*-GFP$^+$ than in CD45$^-$ *Nes*-GFP$^-$ cells, tenfold higher than in primary osteoblasts and undetectable in osteoclasts (Fig. 1h). Expression of angiopoietin-1 was also several-fold higher in *Nes*-GFP$^+$ cells than in CD45$^-$ *Nes*-GFP$^-$ cells or mature osteoblasts (Supplementary Fig. 5). Therefore, these results indicated that *Nes*-GFP$^+$ cells met the requirements (for example, innervated cell expressing Cxcl12)[18] for a candidate stromal cell regulating steady-state HSC traffic.

Nestin$^+$ cells co-localize with HSCs in the bone marrow

To evaluate the spatial relationships between *Nes*-GFP$^+$ cells and HSCs, we immunostained femoral sections of *Nes-Gfp* transgenic mice for haematopoietic lineage markers (anti-Ter119, Gr-1, CD3e, B220 and Mac-1), CD48 and CD150. In agreement with previous studies[14], CD150$^+$CD48$^-$Lin$^-$ HSCs represented a very rare subset (~0.005%) of bone marrow nucleated cells. Despite the rarity of both HSCs and *Nes*-GFP$^+$ cells, the vast majority (88%; 37 out of 42) of CD150$^+$CD48$^-$Lin$^-$ cells were located within five cell diameters from *Nes*-GFP$^+$ cells, and most (60%; 25 out of 42) were directly adjacent to previously associated with parathormone administration[1,3] could be due to expansion of nestin$^+$ MSCs rather than mature osteoblasts.

Expression and regulation of HSC maintenance genes

To gain more insight into the regulation of the HSC niche by G-CSF and the SNS, we analysed the expression of genes that regulate HSC maintenance and attraction in the bone marrow[18] (*Cxcl12*, c-kit ligand, angiopoietin-1, interleukin-7, vascular cell adhesion molecule-1 and osteopontin) in mice treated with G-CSF or β-AR agonists. The expression of these genes was extremely high (close to or higher than *Gapdh*) in *Nes*-GFP$^+$ cells, and—with the exception of *Angpt1*—50–700-fold higher than in the other bone marrow stromal cells.

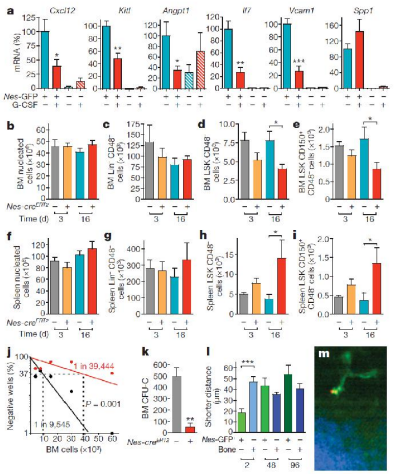

Figure 4 | Regulation of HSC maintenance by nestin$^+$ MSCs. a, Expression and regulation of core HSC maintenance genes by CD45$^-$ *Nes*-GFP$^+$ cells. Q-PCR for *Cxcl12*, stem cell factor/kit ligand (*Kitl*), angiopoietin-1 (*Angpt1*), interleukin-7 (*Il7*), vascular cell adhesion molecule-1 (*Vcam1*) and osteopontin (*Spp1*) in CD45$^-$ *Nes*-GFP$^+$ and CD45$^-$ *Nes*-GFP$^-$ cells sorted from the bone marrow of mice injected with G-CSF or vehicle ($n = 6$). **b–k**, Bone marrow (BM) and spleen nucleated (**b**, **f**), Lin$^-$ CD48$^-$ (**c**, **g**), CD48$^-$ LSK (**d**, **h**) and CD150$^+$CD48$^-$ LSK (**e**, **i**) cells 3–16 days after tamoxifen and diphtheria toxin administration in *Nes-cre^{ERT2}iDTR* double- and control *iDTR* single-transgenic mice ($n = 6$–12). **j**, Long-term culture-initiating cell assay using limiting dilutions of bone marrow cells from *Nes-cre^{ERT2}iDTR* (red) or control *iDTR* mice (black) 1 month after tamoxifen and diphtheria toxin treatment; the percentage of culture dishes in each experimental group that failed to generate colony-forming units is plotted against the number of test bone marrow cells; bone marrow HSC frequencies are indicated; Pearson chi-squared test ($n = 4$–6). **k–m**, Nestin$^+$ cells are required for the homing of haematopoietic stem and progenitor cells. **k**, Bone marrow homing of haematopoietic progenitors (CFU-C) in tamoxifen- and diphtheria-toxin-treated *Nes-cre^{ERT2}iDTR* and control *iDTR* mice ($n = 4$–8). **l**, **m**, HSCs rapidly home near GFP$^-$ cells in the bone marrow of *Nes-Gfp* transgenic mice. **l**, Average shorter distances between bone marrow HSCs, *Nes*-GFP$^+$ cells and the bone surface 2 h ($n = 16$), 48 h ($n = 30$) and 96 h ($n = 14$) after HSC transplantation into lethally irradiated mice. **m**, Representative DyD-stained (red) HSC, *Nes*-GFP$^+$ (green) cell and bone matrix (blue). $^*P < 0.05$, $^{**}P < 0.01$, $^{***}P < 0.001$; unpaired two-tailed *t*-test. All error bars indicate s.e.m.

Moreover, these genes, except osteopontin, were significantly and selectively downregulated in *Nes*-GFP$^+$ cells by G-CSF (Fig. 4a) or β_3-AR agonists (Supplementary Fig. 14a). Very similar results were obtained when β-actin was used as a housekeeping gene instead of *Gapdh* (Supplementary Fig. 15). The expression of connexin-45 and connexin-43 was also 200–500-fold higher in *Nes*-GFP$^+$ cells than in CD45$^-$ *Nes*-GFP$^-$ cells (Supplementary Fig. 14b), indicating the existence of electromechanical coupling involving nestin$^+$ cells innervated by noradrenergic nerve terminals[16,18,19].

Nestin$^+$ cells maintain HSCs in the bone marrow

To determine whether nestin$^+$ cells are required for HSC maintenance in the bone marrow, we performed selective depletion experiments by intercrossing a Cre-recombinase-inducible diphtheria toxin receptor line[39] (*iDTR*) with *Nes-cre^{ERT2}* mice. In adult *Nes-cre^{ERT2}iDTR* mice, tamoxifen and diphtheria toxin treatment severely reduced bone marrow nestin$^+$ cells, as estimated by mesensphere-forming efficiency (92.9 ± 1.8% reduction; $n = 6$). Whereas bone marrow cellularity and Lin$^-$ CD48$^-$ cell numbers were not affected in *Nes-cre^{ERT2}iDTR* mice up to 2 weeks after treatment with diphtheria toxin (Fig. 4b, c), the more immature CD48$^-$ Lin$^-$ Sca-1$^+$ c-kit$^+$ (LSK) cells (Fig. 4d) and CD150$^+$ CD48$^-$ LSK cells (Fig. 4e) were reduced by ~50%. This was associated with a proportional and selective increase in the number of LSK and CD150$^+$CD48$^-$ LSK cells in the spleen (Fig. 4f–i), without detectable difference in cell cycle profile or apoptotic rates (Supplementary Fig. 16). Moreover, long-term culture-initiating cell (LT-CIC) assay using limiting dilutions of bone marrow cells obtained from *Nes-cre^{ERT2}iDTR* double transgenic or control *iDTR* mice 1 month after tamoxifen and diphtheria toxin treatment showed a ~4-fold reduction in bone marrow HSC activity after depletion of nestin$^+$ cells (Fig. 4j). Thus, these studies indicate that HSCs/progenitors are reduced in the bone marrow after the depletion of nestin$^+$ cells, owing at least in part to mobilization towards extramedullary sites.

Nestin$^+$ cells are required for HSC/progenitor homing

To evaluate further the impact of nestin$^+$ cells in progenitor trafficking to bone marrow, we assayed haematopoietic progenitor homing to the bone marrow, and found it to be markedly reduced (by 90%) in diphtheria-treated, lethally irradiated *Nes-cre^{ERT2}iDTR* mice (Fig. 4k). To assess more specifically the homing of HSCs, we tracked by intravital microscopy highly purified, fluorescently labelled HSCs after transplantation into lethally irradiated *Nes-Gfp* transgenic mice, as described[40]. Calvarial *Nes*-GFP$^+$ cells were also perivascular (Supplementary Fig. 17), contained all colony-forming units-fibroblast (CFU-F) and sphere-forming cells (data not shown). Analyses of average shorter distances of homed HSCs from *Nes*-GFP$^+$ cells and the bone surface revealed that HSCs rapidly home near *Nes*-GFP$^+$ cells in the bone marrow (Fig. 4l, m), indicating that bone marrow nestin$^+$ cells participate in directed HSC migration.

Discussion

These studies indicate that nestin$^+$ cells represent bona fide niche cells in that they show a close physical association with HSCs, very high expression levels of core HSC maintenance genes, selective down-regulation of these genes by G-CSF or β3-AR stimulation, and significant reductions in bone marrow HSCs upon their deletion. In addition, they behave functionally as MSCs based on their exclusive CFU-F content, multilineage differentiation towards mesenchymal lineages, robust self-renewal in serial transplantation and *in vivo* contribution to osteochondral lineages under homeostasis. Furthermore, we provide evidence for a balanced regulation of haematopoietic and mesenchymal lineages at the stem-cell level where homeostatic neural (for example, SNS) and hormonal (for example, parathormone) mechanisms tightly regulate in tandem HSC maintenance and MSC proliferation and differentiation.

[1]Department of Medicine, Mount Sinai School of Medicine, New York, New York 10029, USA. [2]Department of Gene and Cell Medicine, Mount Sinai School of Medicine, New York, New York 10029, USA. [3]Cold Spring Harbor Laboratory, Cold Spring Harbor, New York 11724, USA. [4]Center for Regenerative Medicine, Massachusetts General Hospital, Harvard Medical School, Boston, Massachusetts 02114, USA. [5]Department of Pharmacology and Systems Therapeutics, Mount Sinai School of Medicine, New York, New York 10029, USA. [6]Ruth L. and David S. Gottesman Institute for Stem Cell and Regenerative Medicine Research, Albert Einstein College of Medicine, Bronx, New York 10461, USA. †Present address: Department of Cardiovascular Developmental Biology, Centro Nacional de Investigaciones Cardiovasculares Carlos III, Madrid 28029, Spain (S.M.-F.); Institute for Life Sciences, University of Southampton, Highfield, Southampton SO17 1BJ, UK (B.D.M.).

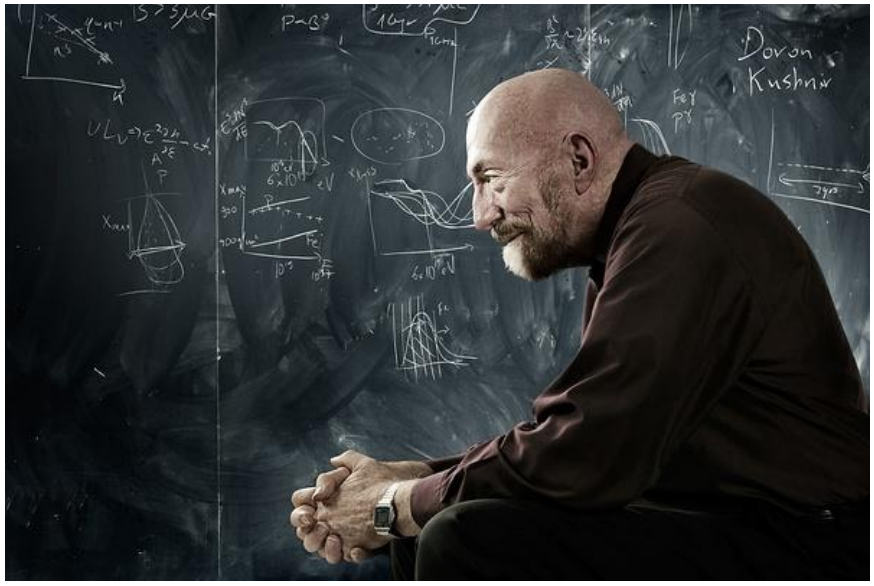
Doron
Kushnir

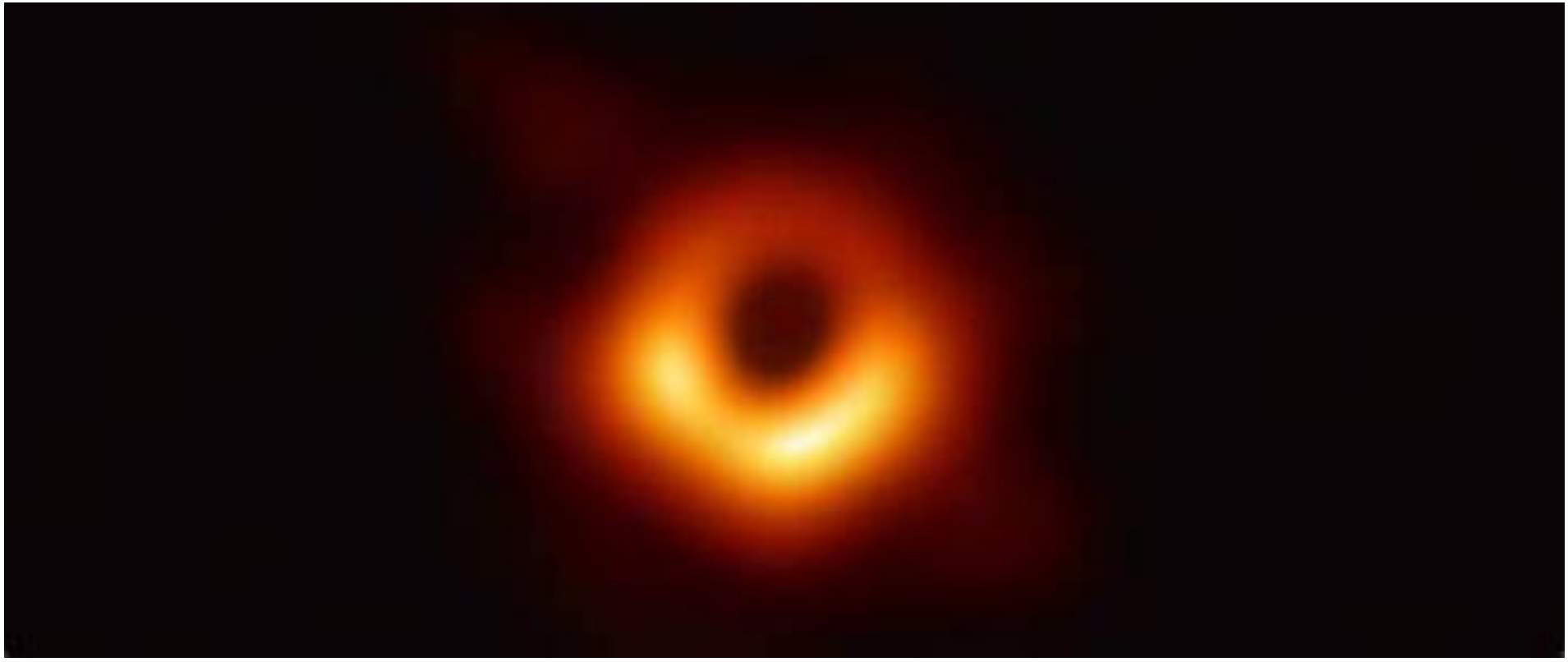

FIGURE QUALITY
IS A PAPER'S
"SUIT AND TIE."

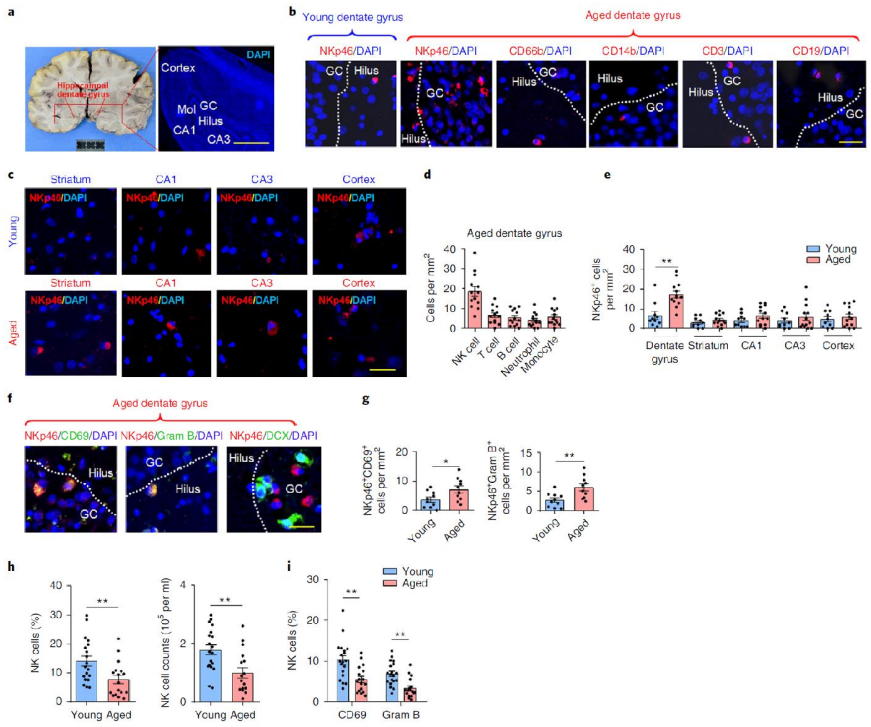

Fig. 1 | Accumulation of NK cells in the dentate gyrus of normal aged human brains. a, Postmortem human brain tissue containing the hippocampal dentate gyrus region. Mol, molecular layer; GC, granule cells. **b**, Left: NK cells (NKp46$^+$) in the dentate gyrus of a young (37 years old) human brain. Right: NK cells (NKp46$^+$), neutrophils (CD66b$^+$), monocytes (CD14$^+$), T cells (CD3$^+$) and B cells (CD19$^+$) in the dentate gyrus of an aged (74 years old) human brain. Dashed lines mark the boundaries between granule cell layer and hilus. **c**, NKp46$^+$ cells in the striatum of a young (37 years old) and an aged (74 years old) human brain. **d**, NK cells outnumber T cells, B cells, neutrophils and monocytes in the aged human dentate gyrus. **e**, Quantification of NK cells in dentate gyrus and striatum areas from young and aged human brain tissues. **f**, NK cells expressing CD69 or granzyme B (Gram B) in an aged human dentate gyrus (74 years old). NKp46$^+$ cells are in close proximity to DCX$^+$ cells. Dashed lines mark the boundaries between granule cell layer and hilus. **g**, Quantification of NK cells expressing CD69 or Gram B in the aged human dentate gyrus. In **d**, **e** and **g**, $n=10$ individuals (male: 5; female: 5) in the young group (30.5 ± 2.6 years); $n=13$ individuals (male: 7; female: 6) in the aged group (71.6 ± 1.5 years). **h**,**i**, Flow cytometry quantification of blood NK cells (**h**) and their expression of CD69 or Gram B (**i**) in young and aged human individuals. In **h** and **i**, $n=19$ individuals (male: 9; female: 10) in the young group (29.8 ± 1.7 years); $n=17$ individuals (male: 9; female: 8) in the aged group (73.5 ± 1.6 years). In **e**, **g**, **h** and **i**, $^*P<0.05$, $^{**}P<0.01$ by two-tailed unpaired Student's *t*-test. **e**, $P=0.0005$, $t=4.111$, d.f. = 21. **g**, left: $P=0.0311$, $t=2.338$, d.f. = 18; right: $P=0.0068$, $t=3.058$, d.f. = 18. **h**, left: $P=0.0089$, $t=2.777$, d.f. = 34; right: $P=0.0027$, $t=3.238$, d.f. = 34. **i**, CD69: $P=0.002$, $t=4.16$, d.f. = 68; Gram B: $P=0.0059$, $t=3.086$, d.f. = 68. Data are representative of three independent experiments. Error bars represent s.e.m. Scale bars, 3 mm (**a**) or 40 μm (**b**, **c** and **f**).

gyrus. In contrast to the intensified NK cell responses in the aged brain, NK cell numbers and their expression of CD69 and granzyme B were reduced in the circulation of aged human individuals relative to young individuals (Fig. 1h,i and Supplementary Fig. 1a). These findings suggest that aging expands NK cells in the brain, which is converse to the contraction observed for NK cells in the periphery.

To further examine how aging affects NK cells in the brain versus the periphery, we enumerated NK cells within various organs from young (3 months old) and aged (18 months old) mice. We found that NK cells accumulate in the aged mouse brain but not in peripheral organs (Fig. 2a,b). Consistent with our findings in the aged human brain, NK cells mainly accumulated in the murine dentate gyrus neurogenic niche during aging (Fig. 2c–f) and were in close proximity to DCX$^+$ dentate gyrus cells (Fig. 2f). In contrast, NK cells were sparse in dentate-gyrus-adjacent areas such as the striatum (Fig. 2d,e). Notably, aging predominantly expanded NK cells

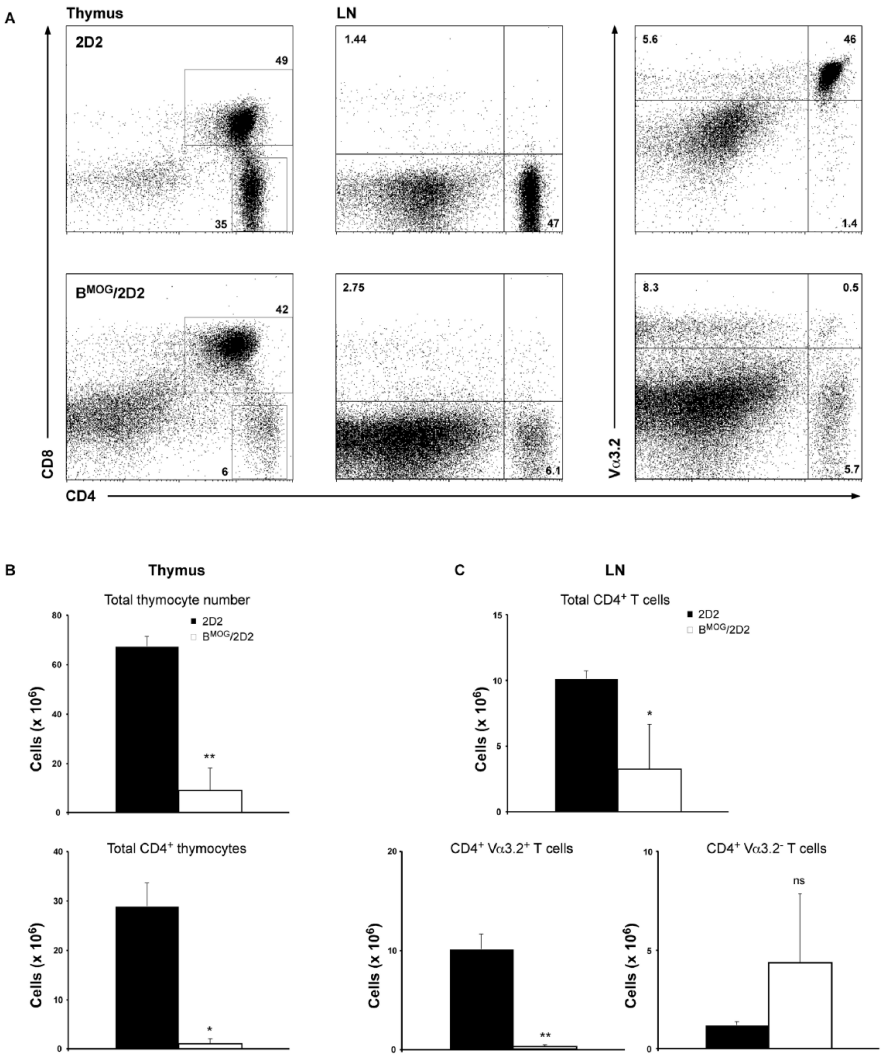

Figure 1. Deletion of 2D2 CD4$^+$ T cells upon MOG encounter by B cells in the thymus. Thymus and LN from WT 2D2 (upper row) and B^{MOG}/2D2 (lower row) mice were analyzed by FACS analysis for presence of CD8$^+$ and CD4$^+$ Va3.2$^+$ T cells, respectively (A). Genotypes and antibodies used are as indicated. Cell surface markers are shown as coordinates. Cells were gated on live lymphocytes. Numbers besides gates or in quadrants indicate percent positive cells in each. Total and CD4 single positive thymocyte numbers (B) and LN total CD4$^+$ as well as CD4$^+$ Va3.2$^+$ and CD4$^+$ Va3.2$^-$ T cell numbers (C) of 2D2 and B^{MOG}/2D2 mice were calculated. Values represent mean ± SEM. ns, not significant.
doi:10.1371/journal.pone.0015372.g001

二 做怎样的图

作图原则

- **清晰，准确，简介，美观**

目标：

- 一看图就能知道文章基本内容，甚至不需要读figure legends；
- 一看图就能知道研究数据质量。

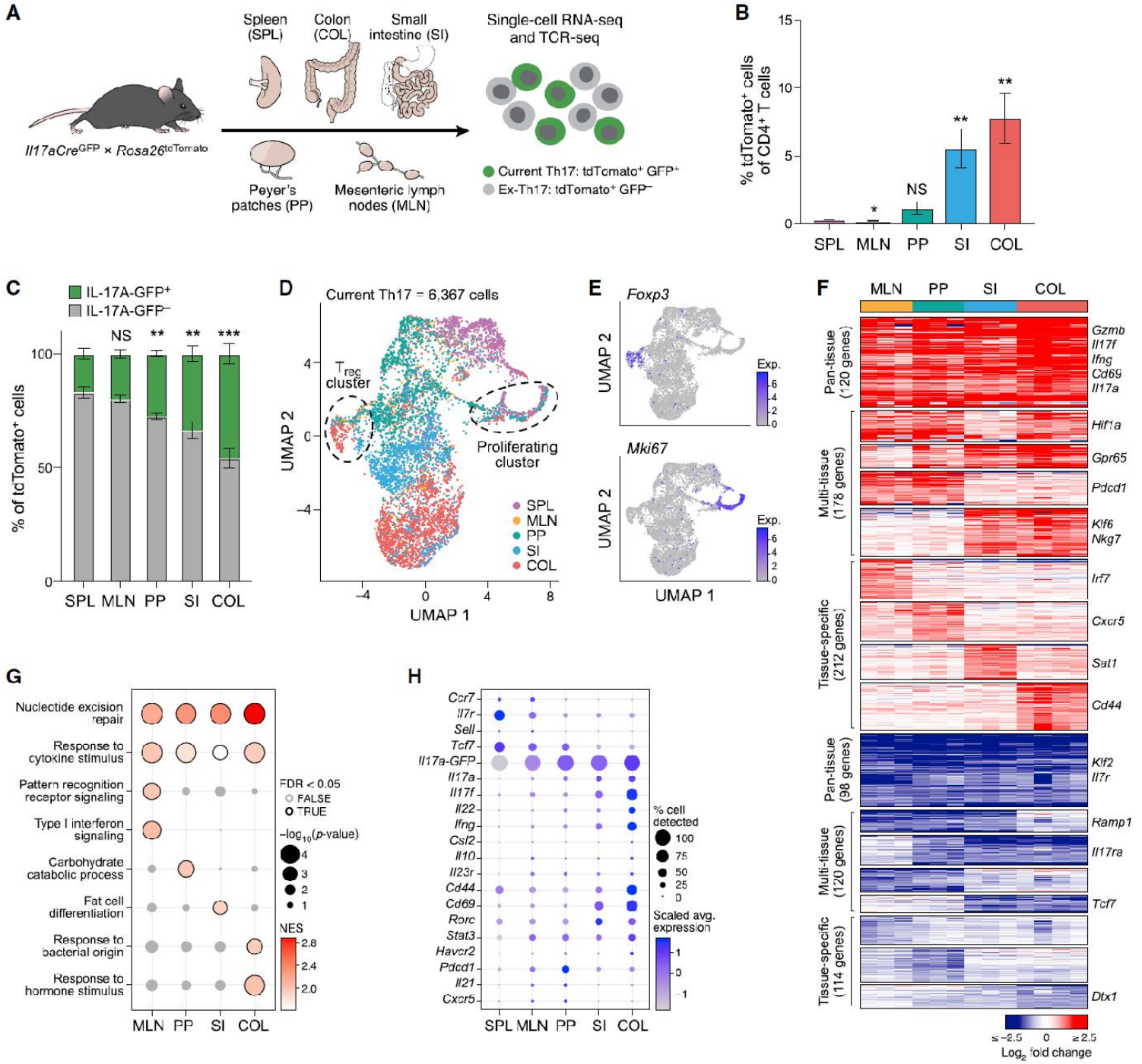
A
Spleen (SPL)
Colon (COL)
Small intestine (SI)
Single-cell RNA-seq and TCR-seq
Il17aCreGFP × Rosa26tdTomato
Peyer's patches (PP)
Mesenteric lymph nodes (MLN)
Current Th17: tdTomato+ GFP+
Ex-Th17: tdTomato+ GFP−
B
% tdTomato+ cells of CD4+ T cells
SPL MLN PP SI COL
C
IL-17A-GFP+
IL-17A-GFP−
% of tdTomato+ cells
D
Current Th17 = 6,367 cells
Treg cluster
Proliferating cluster
UMAP 1
UMAP 2
E
Foxp3
Mki67
Exp.
F
MLN PP SI COL
Pan-tissue (120 genes)
Multi-tissue (178 genes)
Tissue-specific (212 genes)
Pan-tissue (98 genes)
Multi-tissue (120 genes)
Tissue-specific (114 genes)
Gzmb
Il17f
Ifng
Cd69
Il17a
Hif1a
Gpr65
Pdcd1
Klf6
Nkg7
Irf7
Cxcr5
Sat1
Cd44
Klf2
Il7r
Ramp1
Il17ra
Tcf7
Dtx1
Log2 fold change
G
Nucleotide excision repair
Response to cytokine stimulus
Pattern recognition receptor signaling
Type I interferon signaling
Carbohydrate catabolic process
Fat cell differentiation
Response to bacterial origin
Response to hormone stimulus
FDR < 0.05
FALSE
TRUE
−log10(p-value)
NES
H
Ccr7
Il7r
Sell
Tcf7
Il17a-GFP
Il17a
Il17f
Il22
Ifng
Csf2
Il10
Il23r
Cd44
Cd69
Rorc
Stat3
Havcr2
Pdcd1
Il21
Cxcr5
% cell detected
Scaled avg. expression

三 如何做好图

技巧篇

- 适当的文字标记，清楚，易理解；
- 合理的布局，排序——体现科学逻辑；
- 避免数据堆砌，展示关键信息；
- 合理使用颜色——防止单调，避免浮夸；
- 适当使用实验设计流程图。

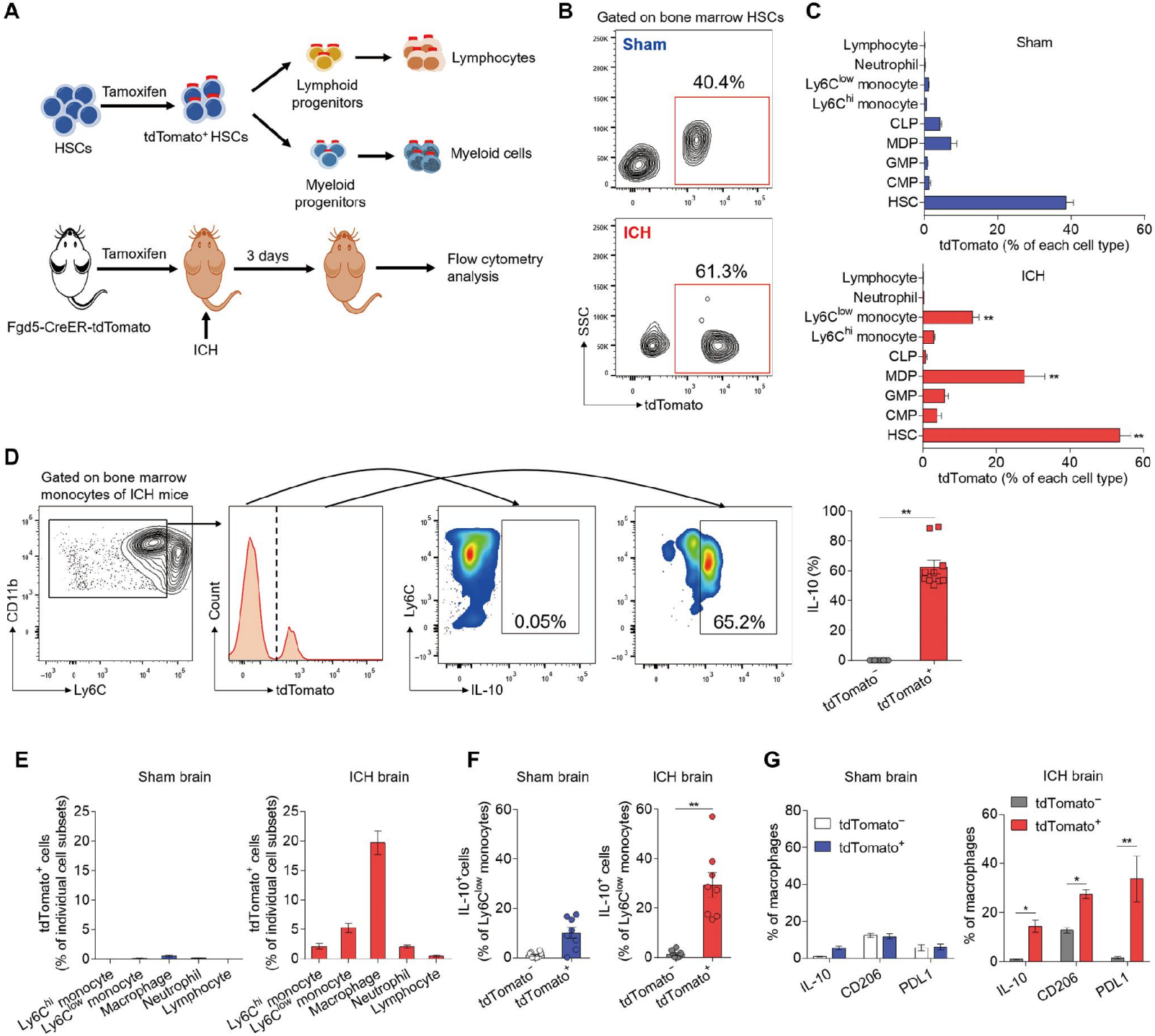
A
Tamoxifen
HSCs
tdTomato+ HSCs
Lymphoid progenitors
Lymphocytes
Myeloid progenitors
Myeloid cells
Tamoxifen
3 days
Flow cytometry analysis
Fgd5-CreER-tdTomato
ICH
B
Gated on bone marrow HSCs
Sham
40.4%
ICH
61.3%
SSC
tdTomato
C
Sham
Lymphocyte
Neutrophil
Ly6Clow monocyte
Ly6Chi monocyte
CLP
MDP
GMP
CMP
HSC
tdTomato (% of each cell type)
ICH
D
Gated on bone marrow monocytes of ICH mice
CD11b
Ly6C
Count
tdTomato
Ly6C
0.05%
65.2%
IL-10
IL-10 (%)
tdTomato−
tdTomato+
E
Sham brain
ICH brain
tdTomato+ cells (% of individual cell subsets)
Ly6Chi monocyte
Ly6Clow monocyte
Macrophage
Neutrophil
Lymphocyte
F
Sham brain
ICH brain
IL-10+cells (% of Ly6Clow monocytes)
IL-10+ cells (% of Ly6Clow monocytes)
tdTomato−
tdTomato+
G
Sham brain
ICH brain
tdTomato−
tdTomato+
% of macrophages
IL-10
CD206
PDL1

分类数据处理经验

流式细胞术

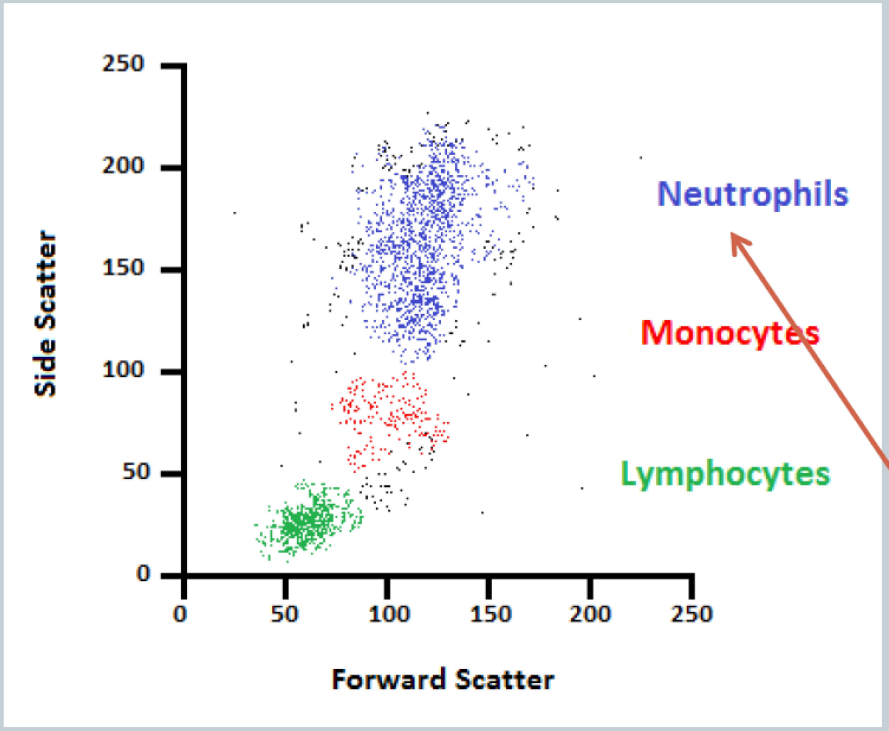

www.labome.com

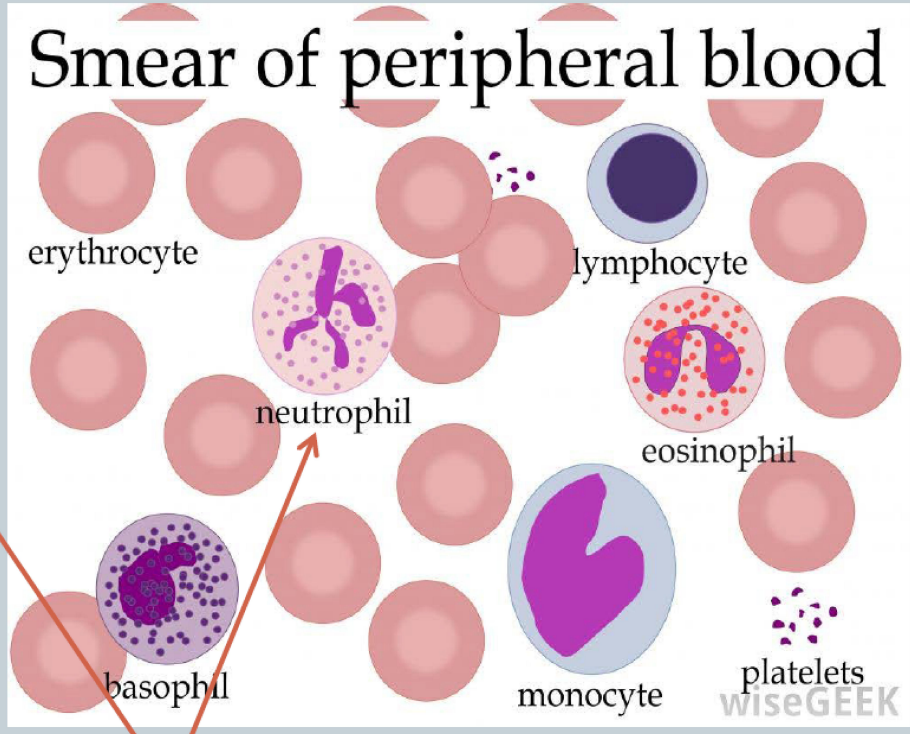

high internal complexity and large size

流式结果呈现

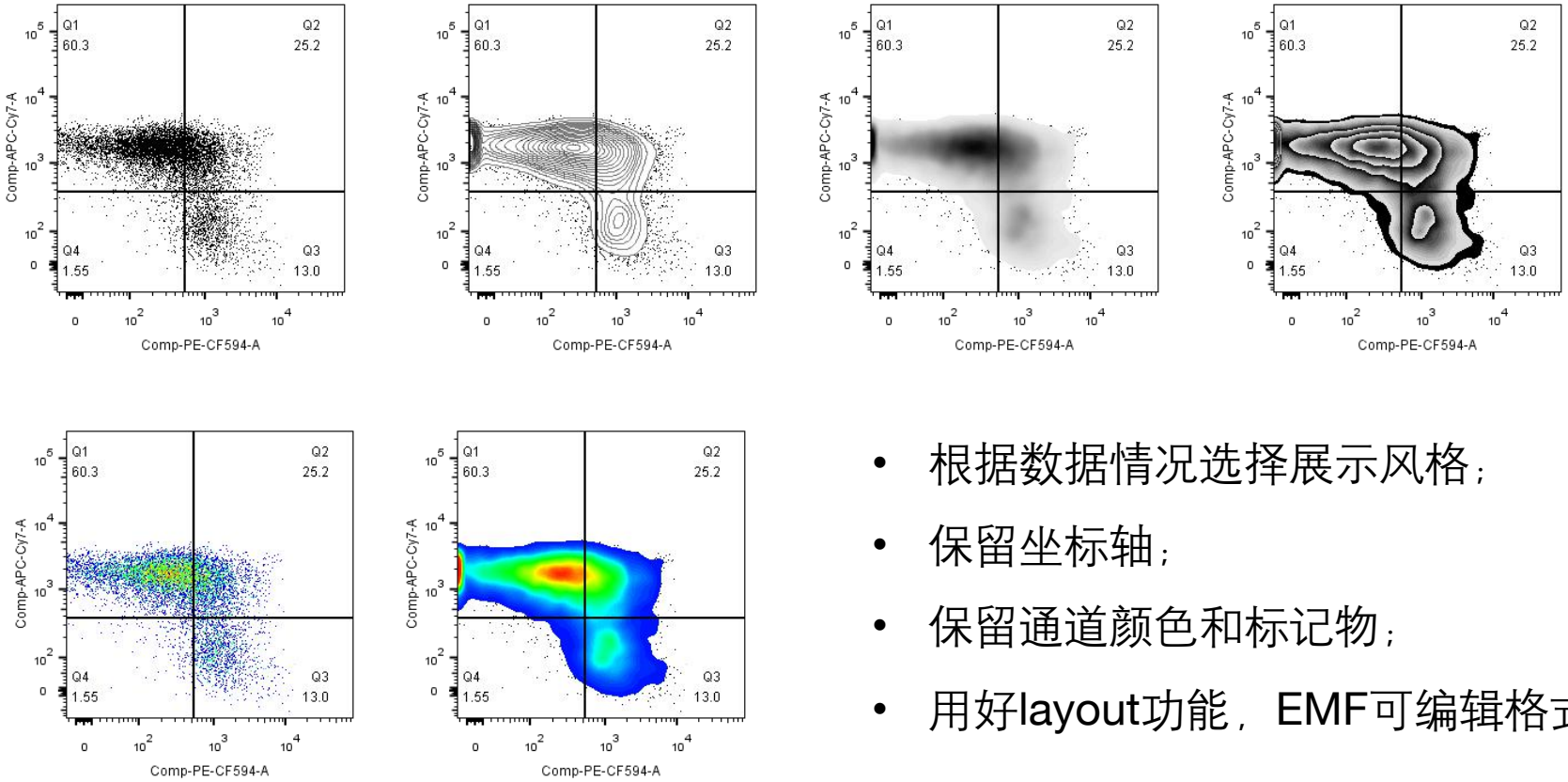

- 根据数据情况选择展示风格；
- 保留坐标轴；
- 保留通道颜色和标记物；
- 用好layout功能，EMF可编辑格式。

- 大多数顶级刊物已不允许使用dot plot

FlowJo 数据传出

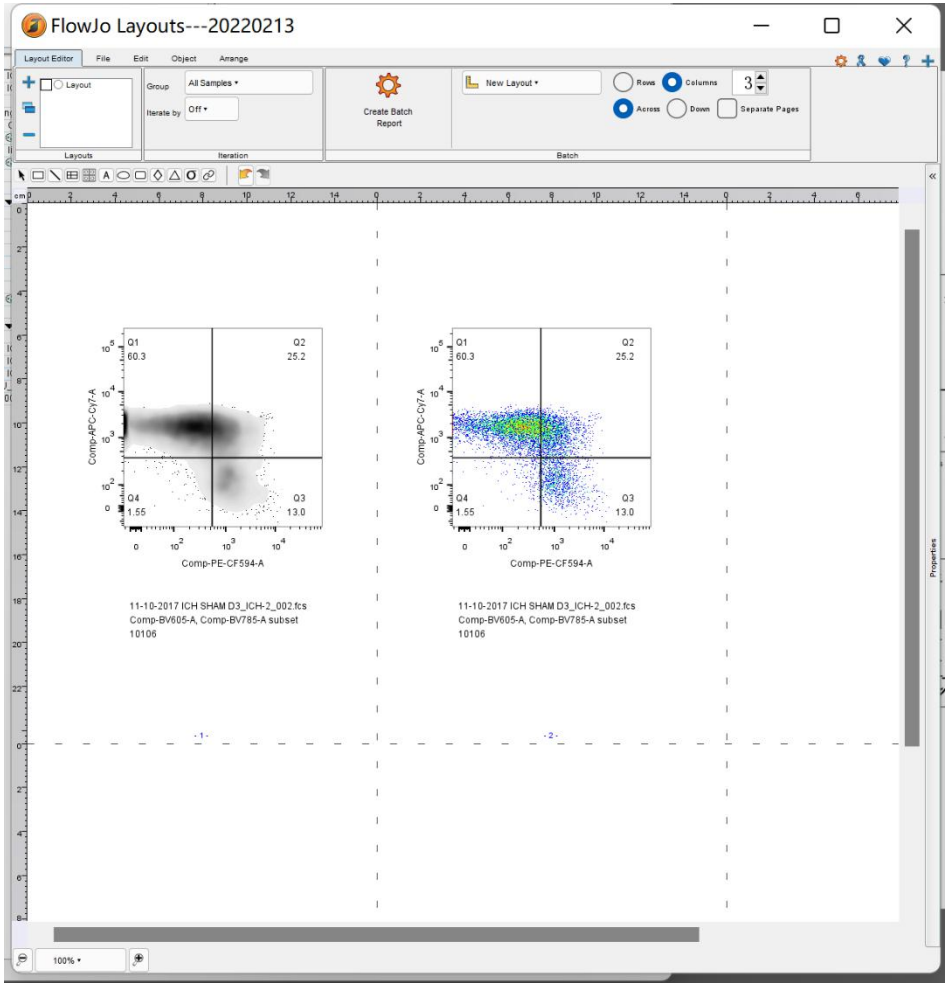
FlowJo Layouts---20220213
Layout Editor
File
Edit
Object
Arrange
Create Batch Report
New Layout
Rows
Columns
Across
Down
Separate Pages
Q1 60.3
Q2 25.2
Q4 1.55
Q3 13.0
Comp-APC-Cy7-A
Comp-PE-CF594-A
11-10-2017 ICH SHAM D3_ICH-2_002.fcs
Comp-BV605-A, Comp-BV785-A subset
10106

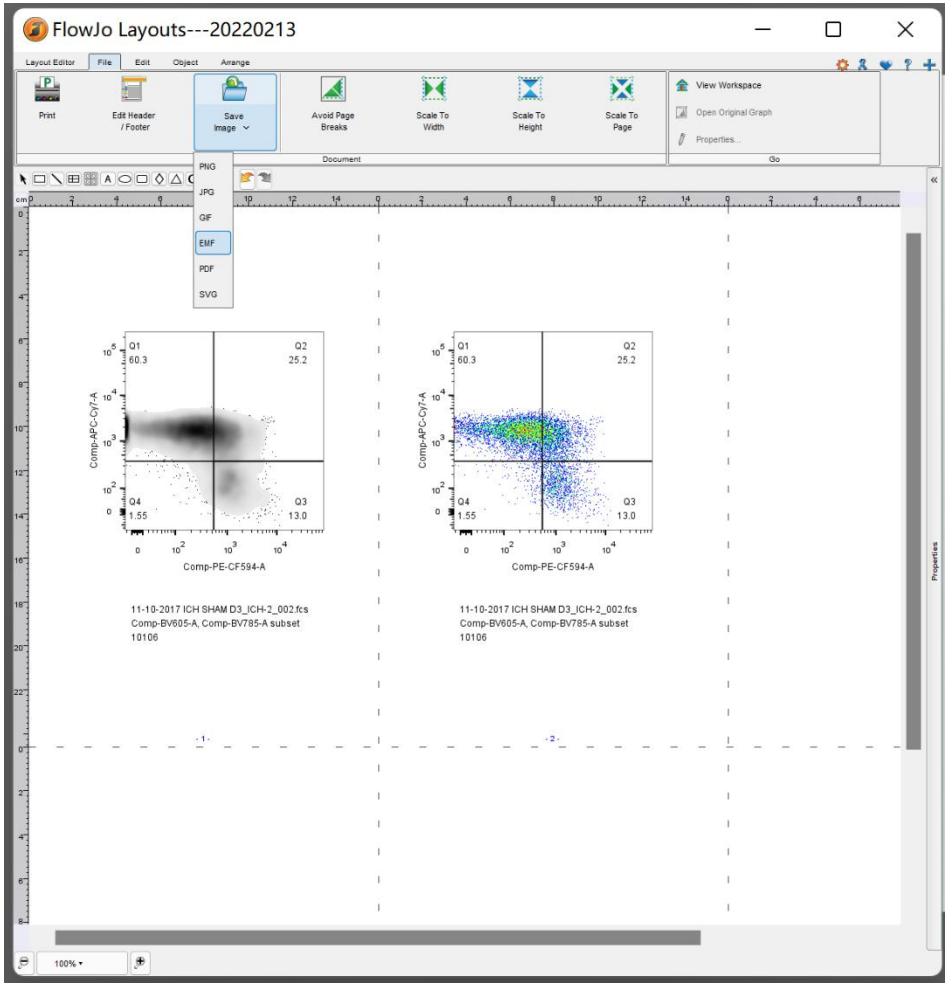
FlowJo Layouts---20220213
Layout Editor
File
Edit
Object
Arrange
Print
Edit Header / Footer
Save Image
Avoid Page Breaks
Scale To Width
Scale To Height
Scale To Page
View Workspace
Open Original Graph
Properties...
PNG
JPG
GIF
EMF
PDF
SVG
Q1 60.3
Q2 25.2
Q4 1.55
Q3 13.0
Comp-APC-Cy7-A
Comp-PE-CF594-A
11-10-2017 ICH SHAM D3_ICH-2_002.fcs
Comp-BV605-A, Comp-BV785-A subset
10106

Back gating

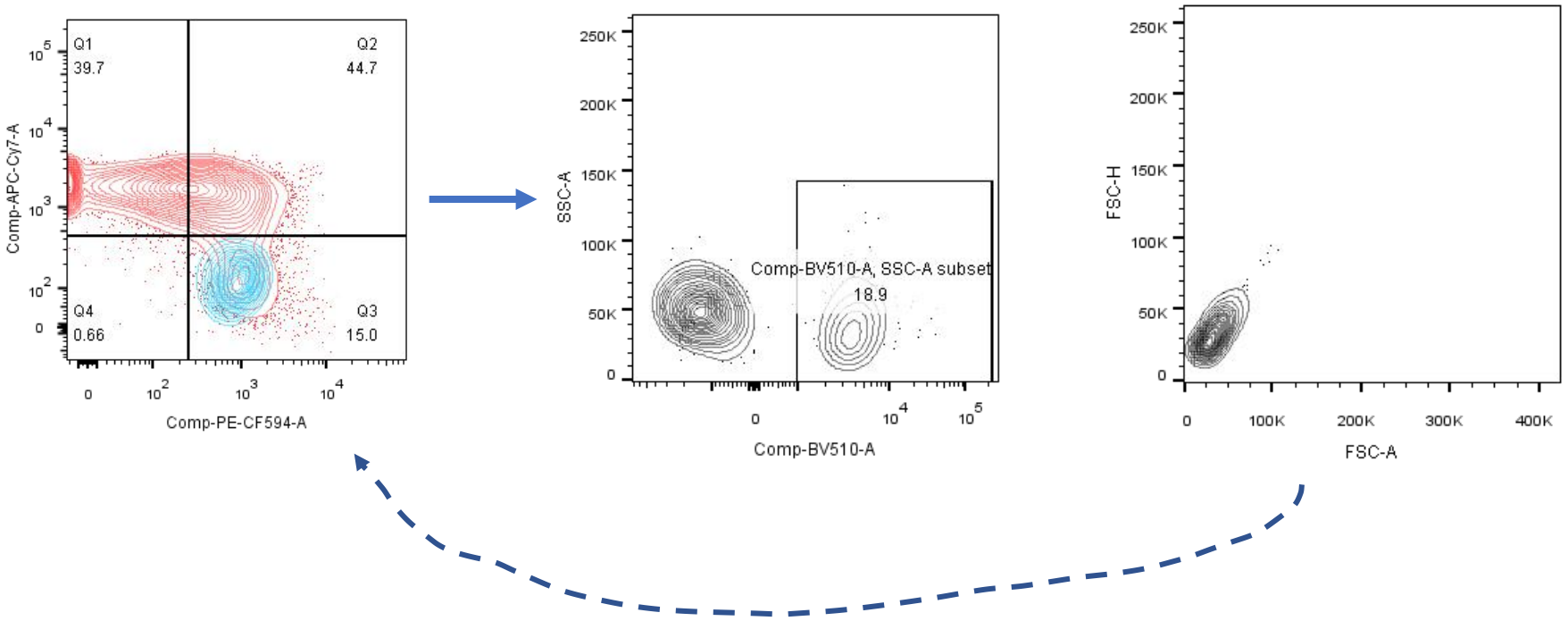
Q1
39.7
Q2
44.7
Q4
0.66
Q3
15.0
Comp-APC-Cy7-A
Comp-PE-CF594-A
SSC-A
Comp-BV510-A, SSC-A subset
18.9
Comp-BV510-A
FSC-H
FSC-A

Flow Histogram

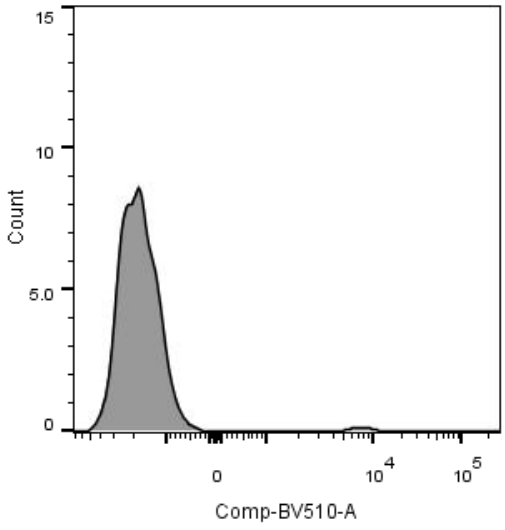

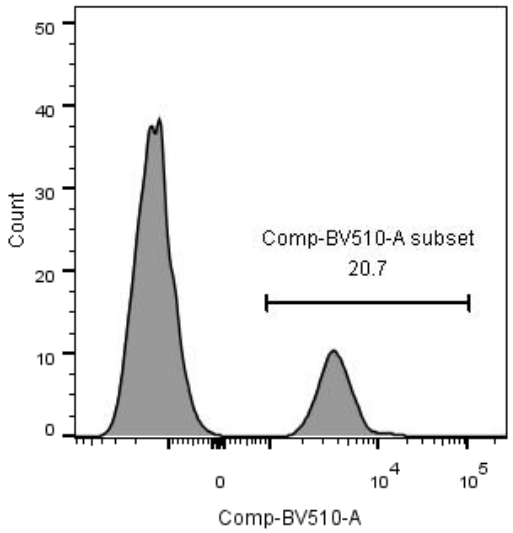

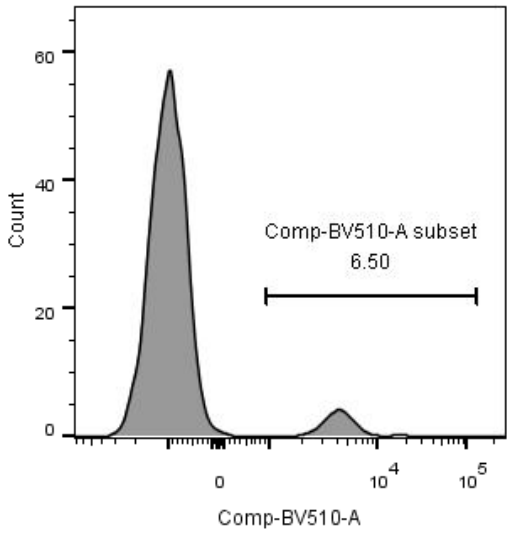

FMO or isotype control;
坐标轴，刻度；

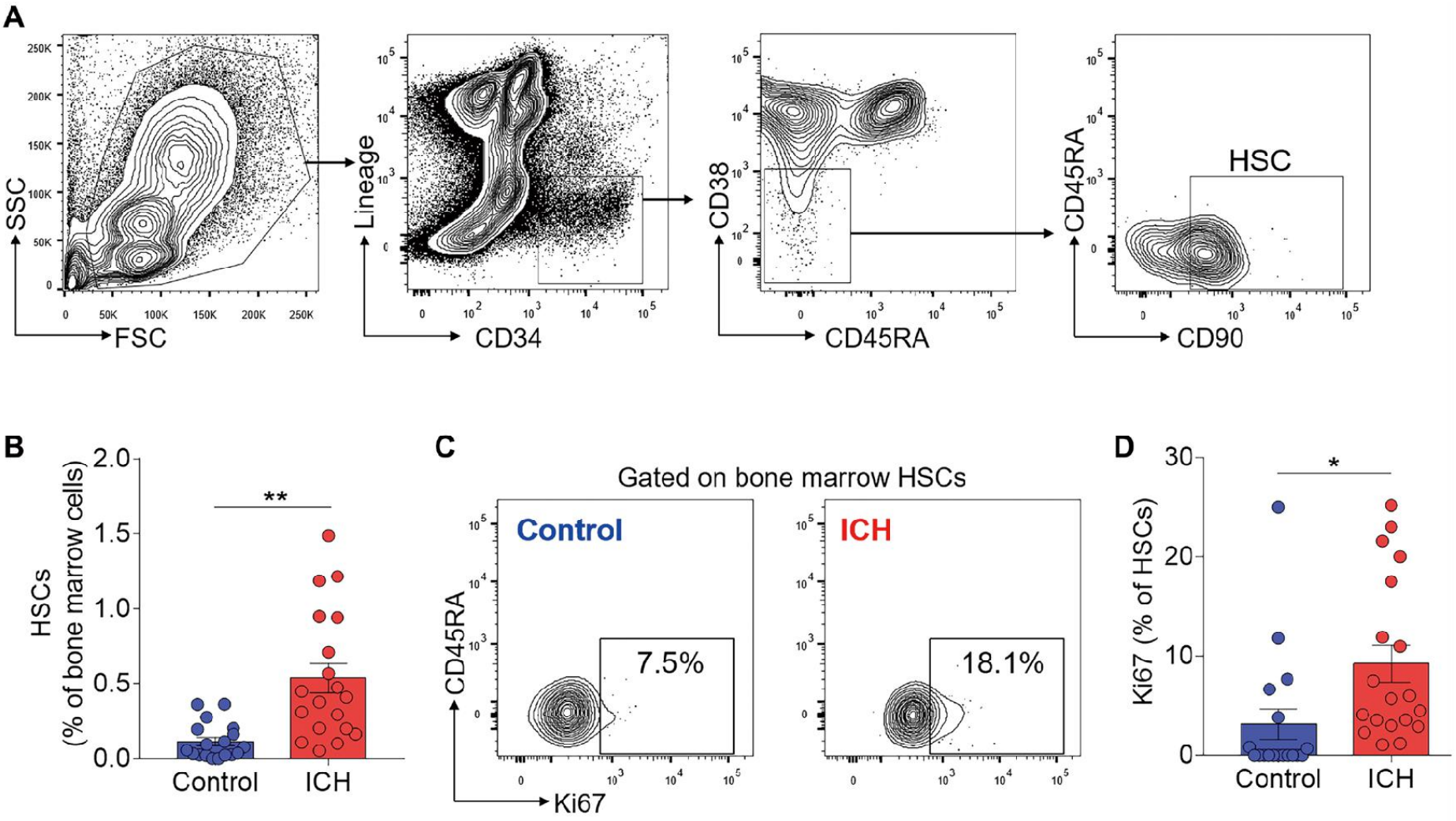

Figure重点：展示gating strategy；标记清楚

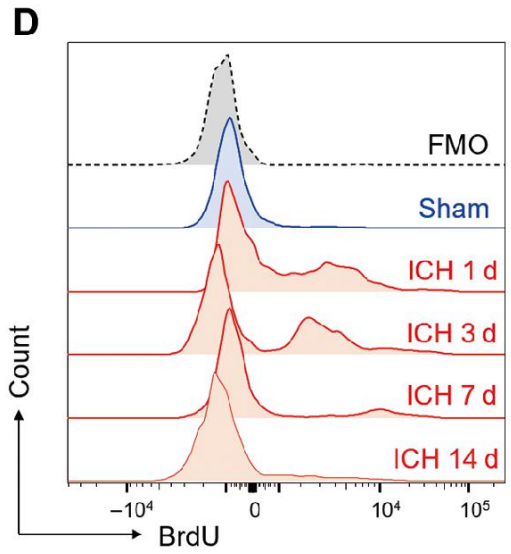

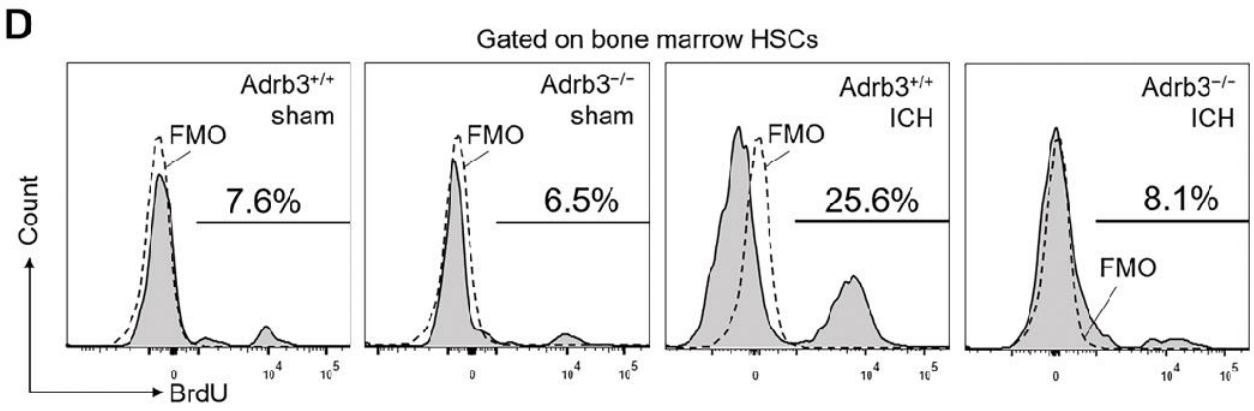

- 同时展示不同组数据；
- 注重阴性对照：FMO/isotype control

流式中文网 已关注

致力于流式细胞术的推广、教育和发展

941篇原创内容 55位朋友关注

星期五 7:10

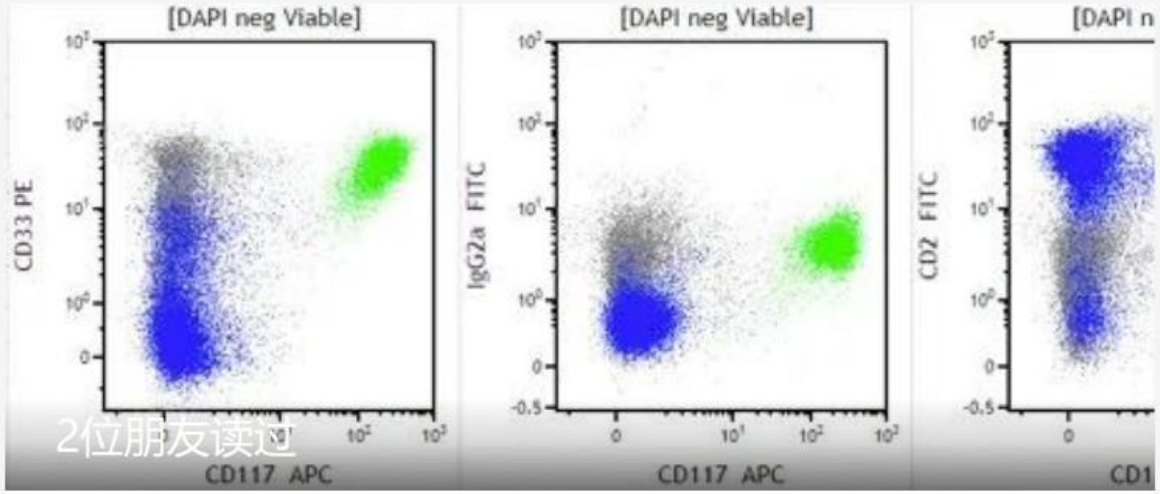

2位朋友读过

肥大细胞免疫表型，以及骨髓实例图

通常，肥大细胞在骨髓中很少见（<1%），在自身免疫和过敏反应时可增高。

病理染色结果

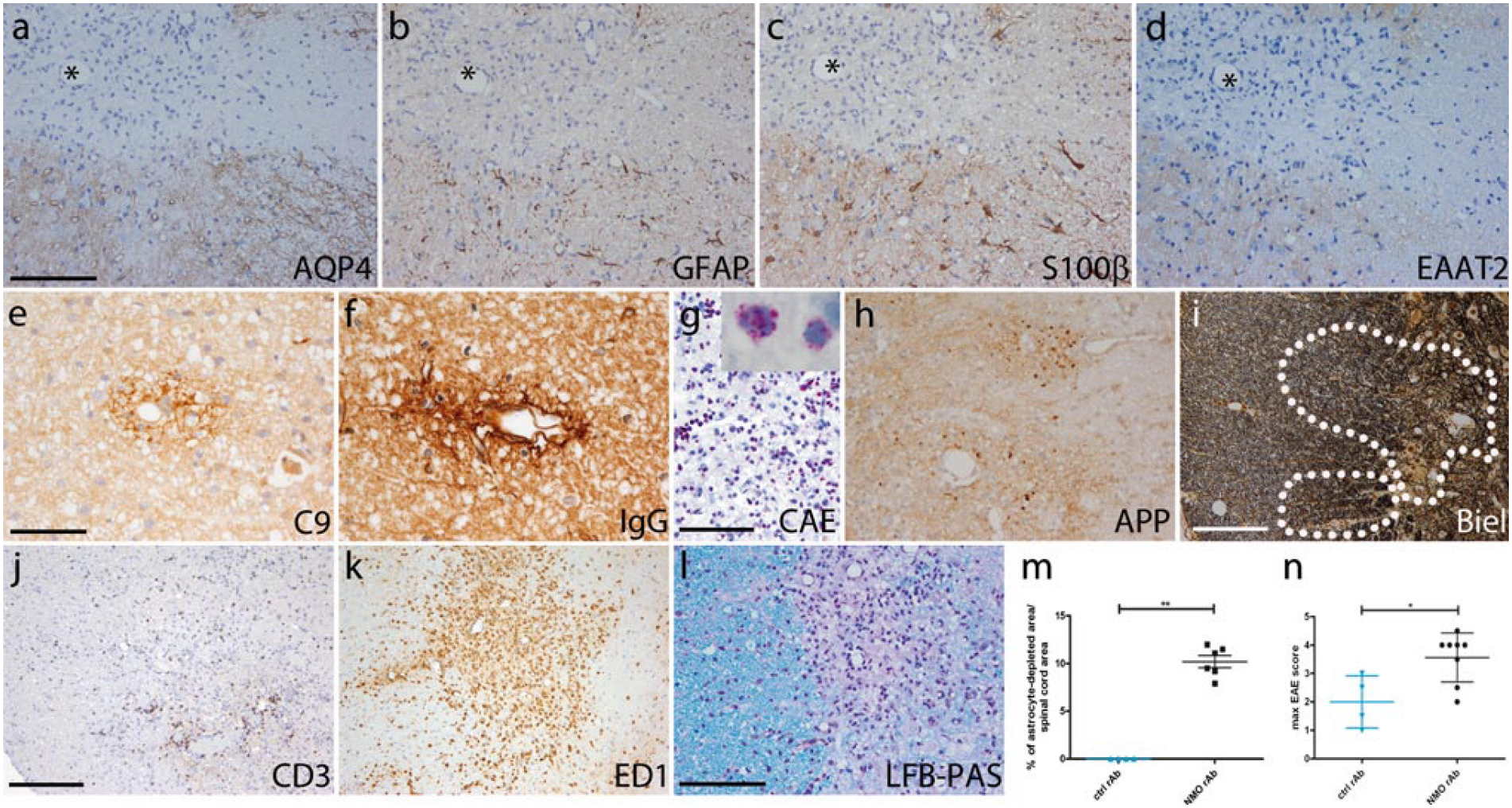

逐一排列，描述病灶病理特征。

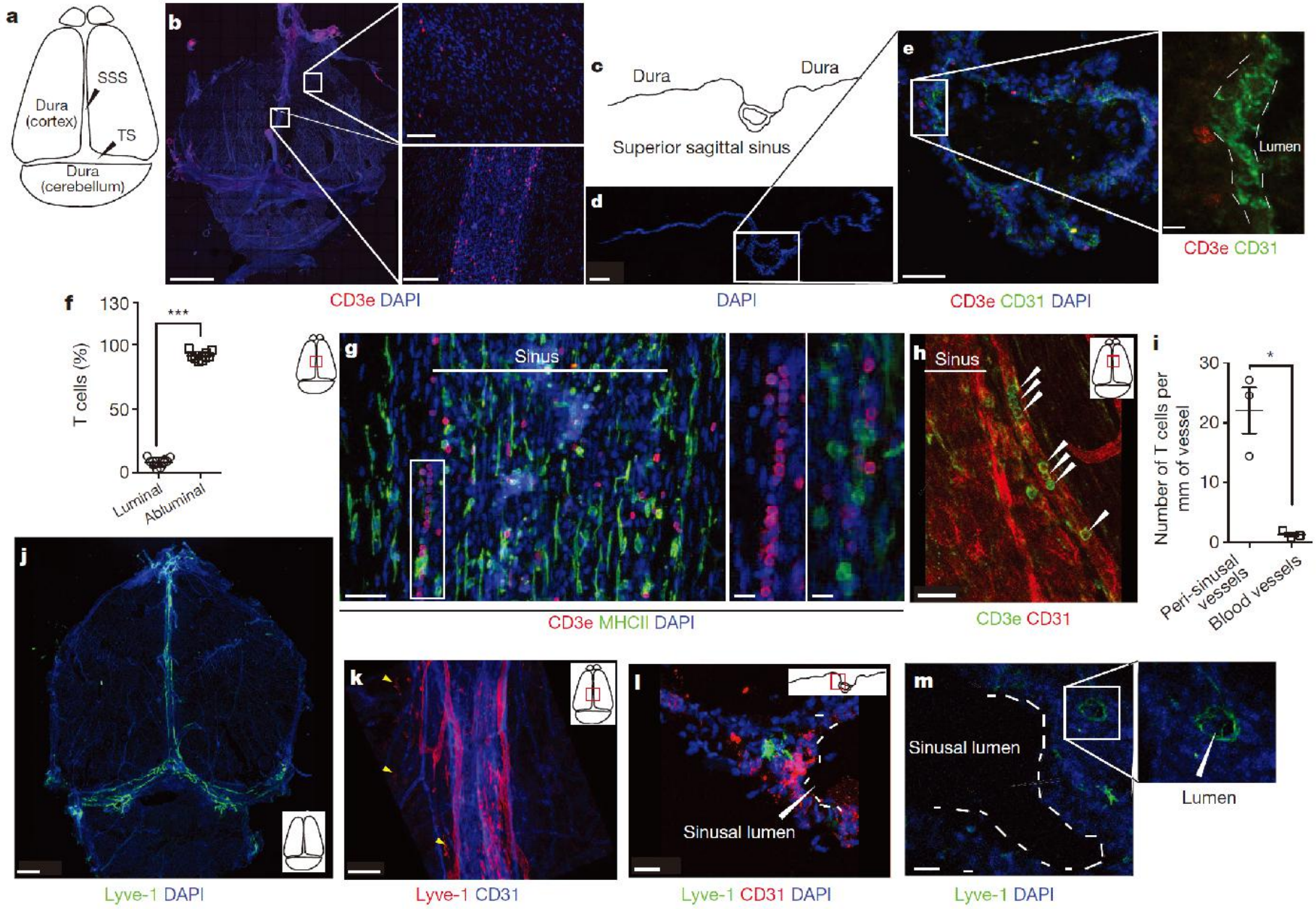
a
SSS
Dura (cortex)
TS
Dura (cerebellum)
b
CD3e DAPI
c
Dura
Dura
Superior sagittal sinus
d
DAPI
e
CD3e CD31 DAPI
Lumen
CD3e CD31
f
130
100
50
0
T cells (%)
***
Luminal
Abluminal
g
Sinus
CD3e MHCII DAPI
h
Sinus
CD3e CD31
i
30
20
10
0
Number of T cells per mm of vessel
*
Peri-sinusal vessels
Blood vessels
j
Lyve-1 DAPI
k
Lyve-1 CD31
l
Sinusal lumen
Lyve-1 CD31 DAPI
m
Sinusal lumen
Lumen
Lyve-1 DAPI

全景呈现+细节刻画

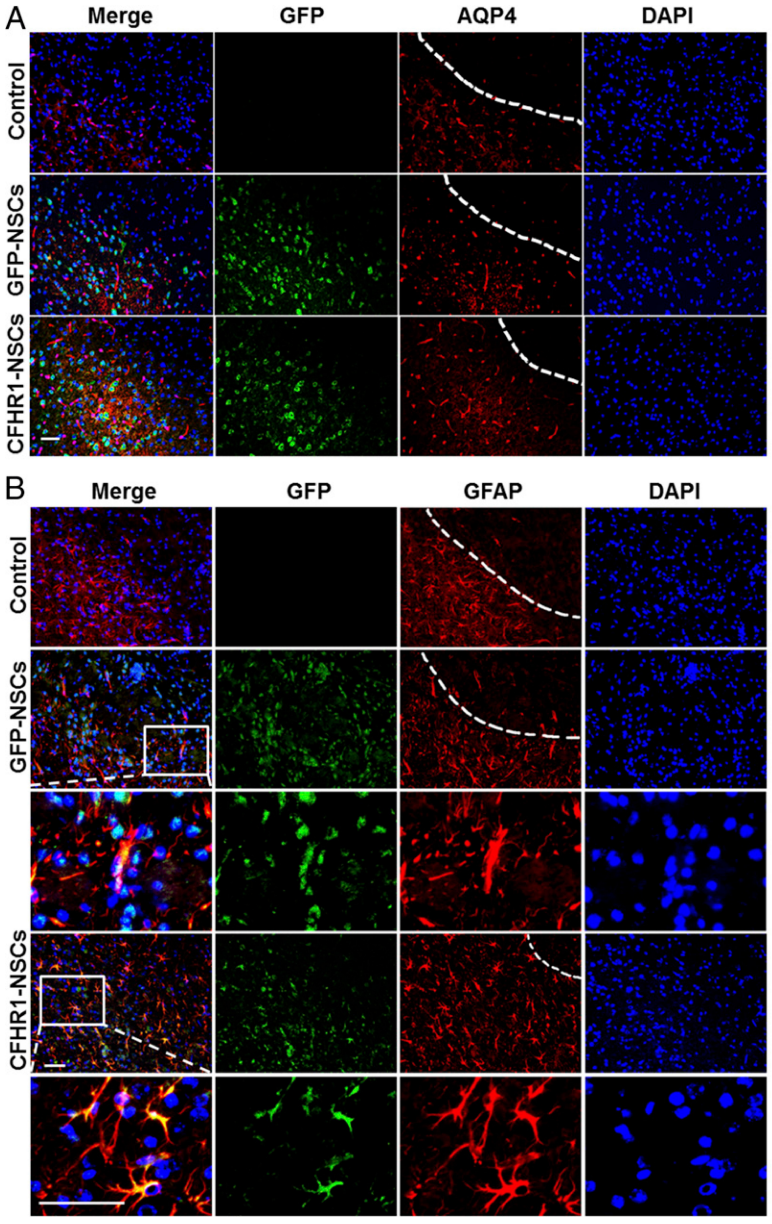

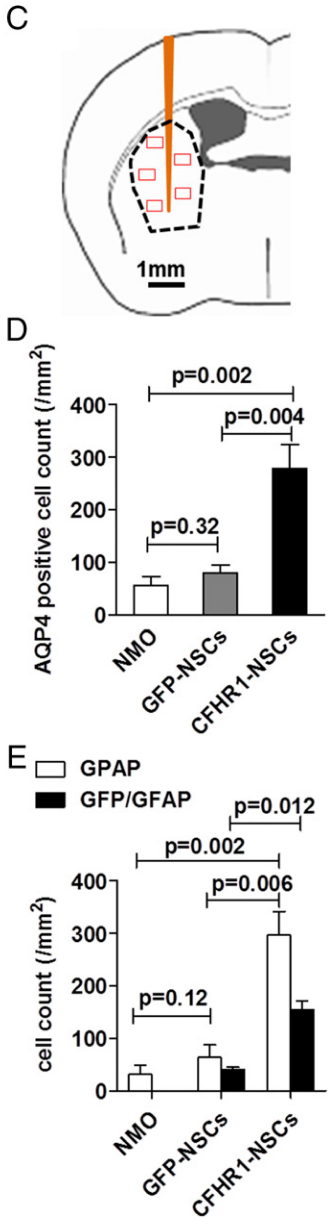

基于病理染色的统计

工具：Iamge J，Image Pro-Plus，Fiji，当心软件骗你

条件：脑区位置，连续层面，统一感兴趣区，同样拍摄条件。

统计图

GraphPad

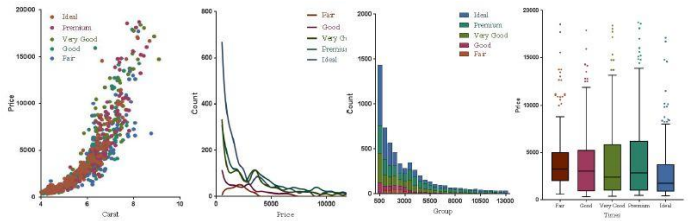

Matlab

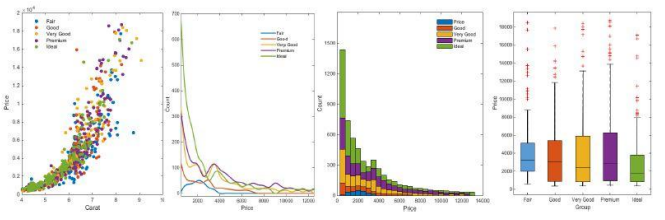

Origin

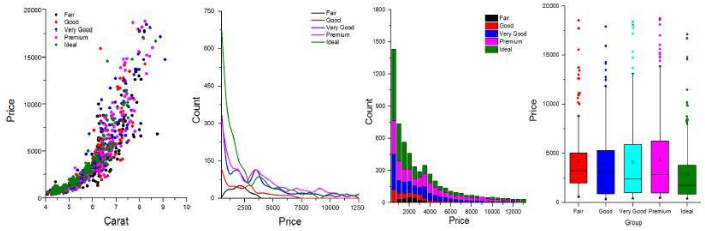

R

ggplot2, lattice, Plotly

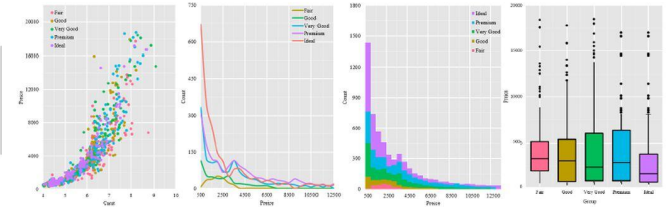

Python

Matplotlib, Seaborn
ggplot, Plotly,
geoplotlib

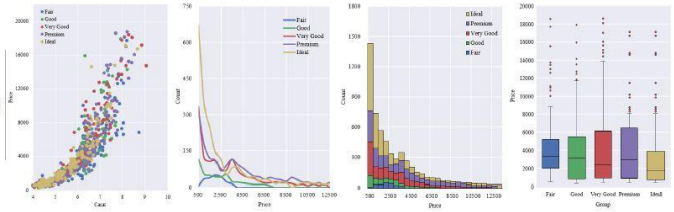

Excel

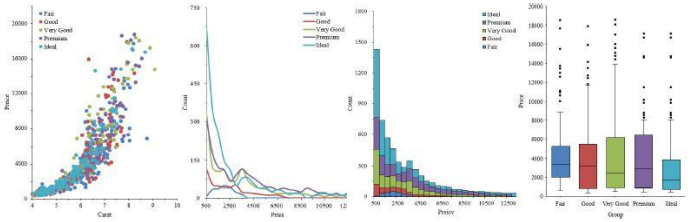

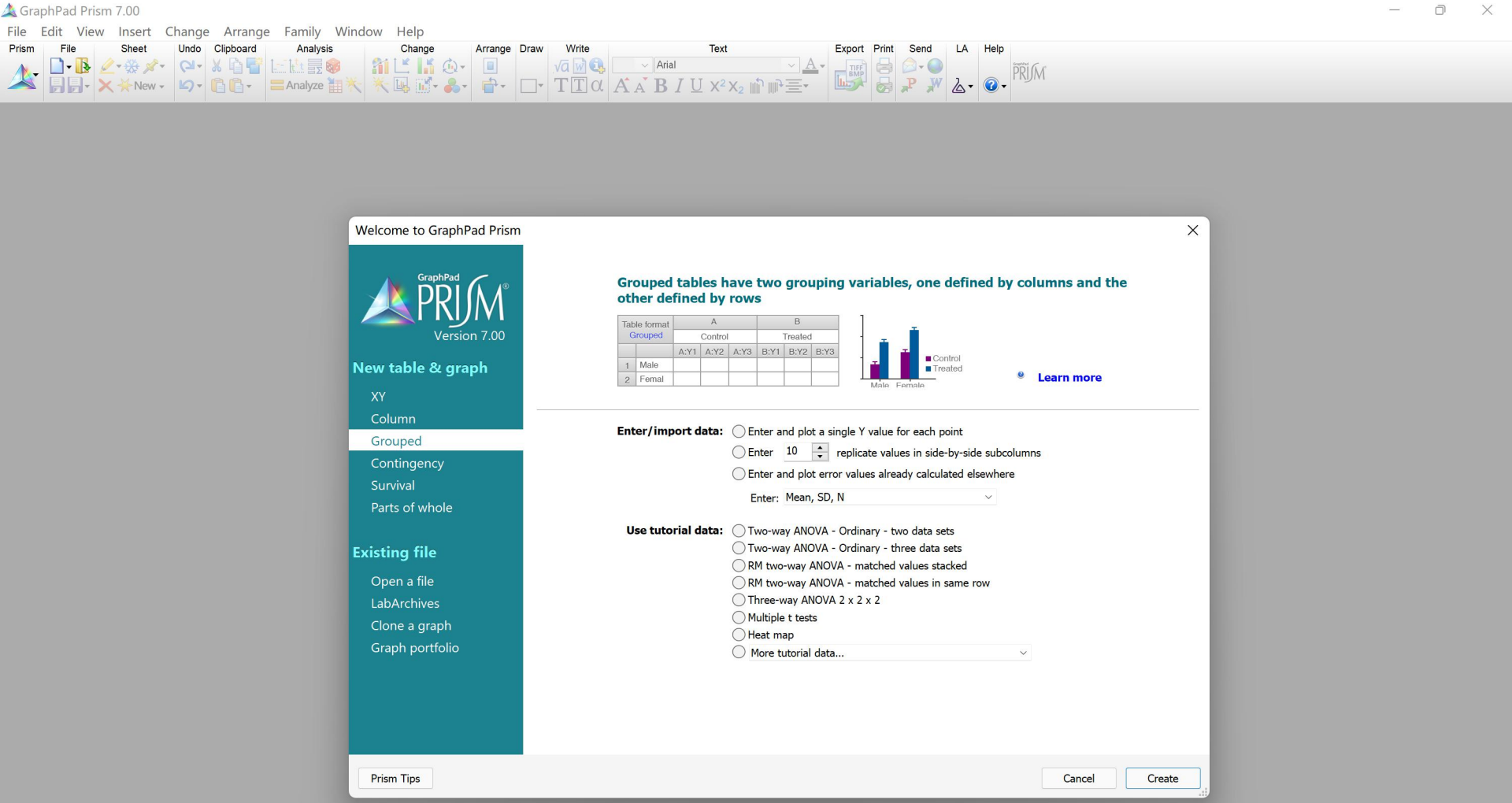

- 集生物统计，曲线拟合和科学绘图于一体，与PPT完美交互；
- 满足几乎所有小样本量统计和绘图。

Tips for using Prism

Expand all tips | Collapse all tips

Getting started tips

- Before using Prism for the first time...
- Pay attention to the distinctions between the eight kinds of data tables
- Learn about the various approaches to making bar graphs
- Recycle your work

Navigation tips

- View all sheets in the gallery
- Jump between related sheets using the Family navigator
- Ping pong (flip back and forth) between two sheets
- Highlight or annotate sheets you want to return to
- Search for sheets

Graphing Tips

- Use the Format Graph and Format Axes dialogs
- Change the color (or size..) of just one symbol or bar
- Use Prism Magic to make graphs consistent
- Change colors by picking a color scheme
- Prism can plot error bars directly from raw data
- To add data to a graph, drag a table from the Navigator and drop onto the graph

Data analysis tips

- Don't run the analysis again -- change the analysis choices
- Use the 'Learn' and 'Analysis checklist' buttons
- Paste results onto your graph
- Create chains of analyses, without copying and pasting

Exporting tips

- Use the Send-to-Word and Send-to-PowerPoint buttons
- Experiment with copying graphs in EMF or WMF format (Windows only)

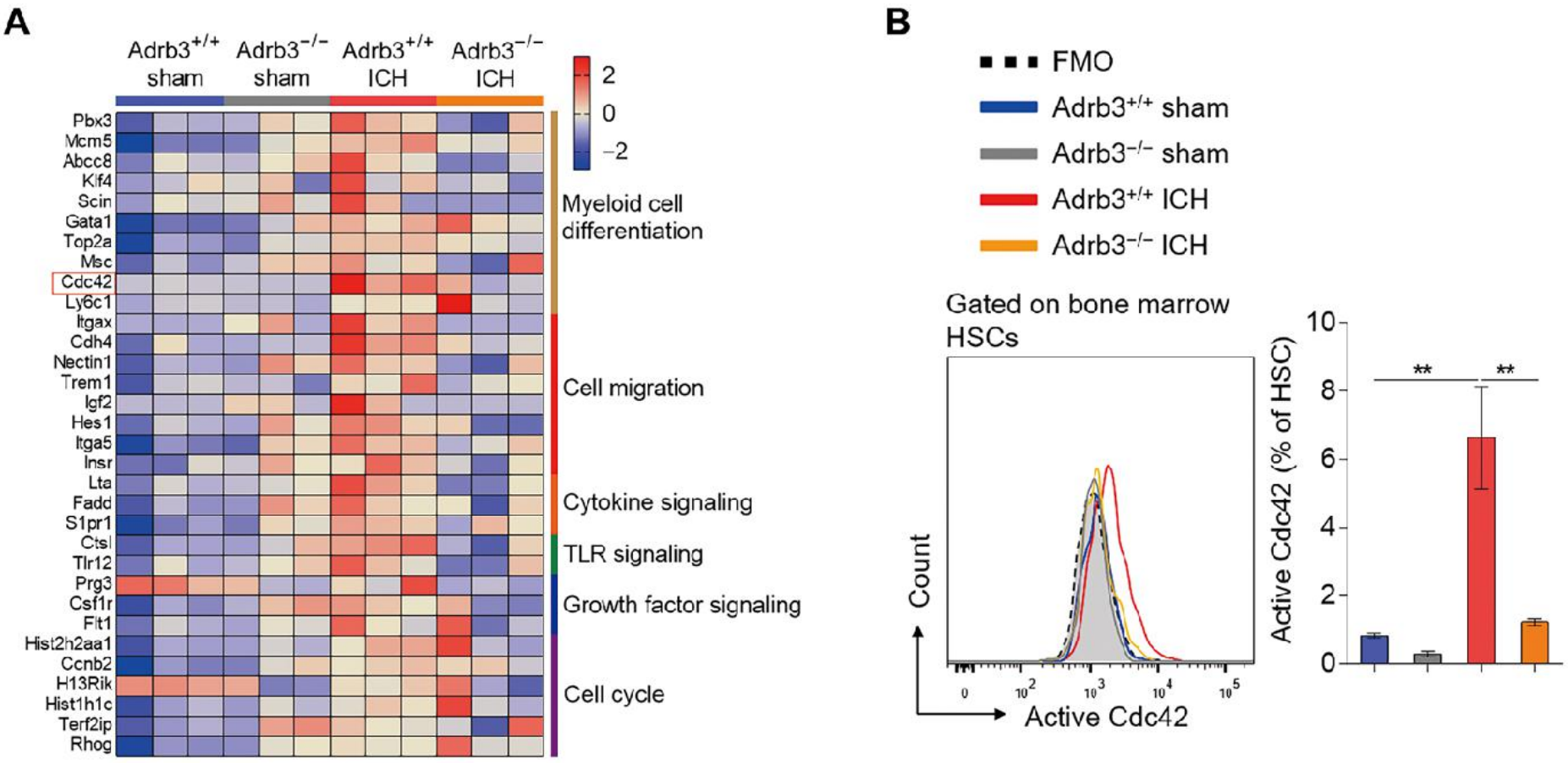

Tips：

所有关于图本身的调整，在graphpad界面完成，不要在ppt里调整图表大小；

一般推荐：arial 14号，为所有文字格式；

不要相信default格式，一般都很丑；

线条粗细，column，dot大小要适宜，过粗显得臃肿。

图表整合

- 工具选择：PPT，AI；
- 一个主题一个图，把不同的图按一条清晰的逻辑线整合到一张图中；
- 作图的同时，要思考结果如何书写。

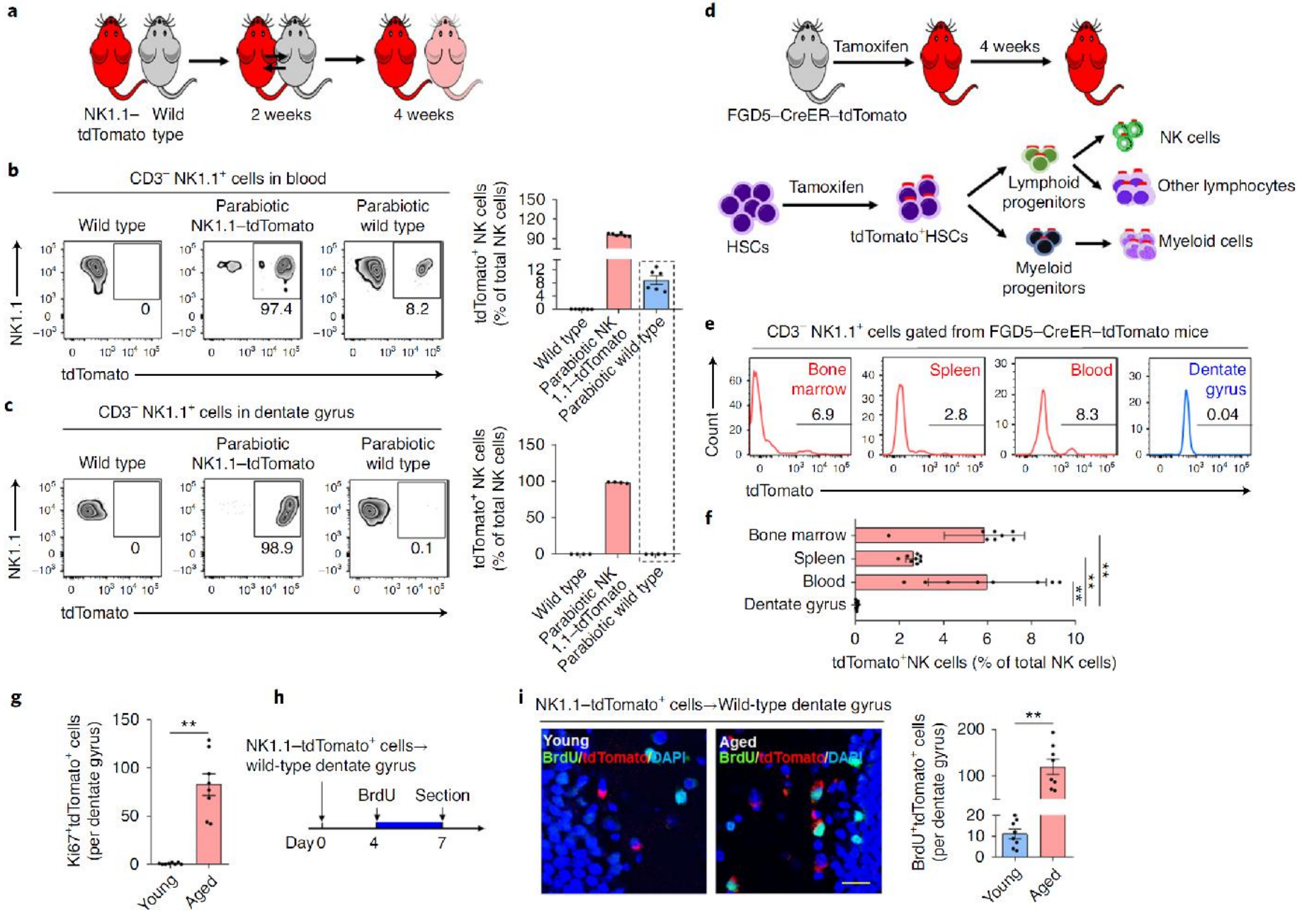
a
NK1.1– tdTomato
Wild type
2 weeks
4 weeks
b
CD3⁻ NK1.1⁺ cells in blood
Wild type
Parabiotic NK1.1–tdTomato
Parabiotic wild type
NK1.1
tdTomato
0
97.4
8.2
tdTomato⁺ NK cells (% of total NK cells)
Wild type
Parabiotic NK 1.1–tdTomato
Parabiotic wild type
c
CD3⁻ NK1.1⁺ cells in dentate gyrus
0
98.9
0.1
d
Tamoxifen
4 weeks
FGD5–CreER–tdTomato
HSCs
tdTomato⁺HSCs
Lymphoid progenitors
Myeloid progenitors
NK cells
Other lymphocytes
Myeloid cells
e
CD3⁻ NK1.1⁺ cells gated from FGD5–CreER–tdTomato mice
Bone marrow
Spleen
Blood
Dentate gyrus
6.9
2.8
8.3
0.04
Count
tdTomato
f
Bone marrow
Spleen
Blood
Dentate gyrus
tdTomato⁺NK cells (% of total NK cells)
g
Ki67⁺tdTomato⁺ cells (per dentate gyrus)
Young
Aged
h
NK1.1–tdTomato⁺ cells→ wild-type dentate gyrus
BrdU
Section
Day 0
4
7
i
NK1.1–tdTomato⁺ cells→Wild-type dentate gyrus
Young
BrdU/tdTomato/DAPI
Aged
BrdU/tdTomato/DAPI
BrdU⁺tdTomato⁺ cells (per dentate gyrus)

四 怎么注释图

Figure legend需要提供哪些信息

- 标题：整个figure 的结论：简明扼要一句话；
- 主要研究对象，实验设计；
- 尽量只解释图反映的是什么实验的什么结果，避免直接描述结果和结论，防止先入为主；
- 结果在图里，结论在读者心里；
- 如果有统计，提供统计学方法，样本量，显著性水平；
- 所有缩写的全称；
- 图，图注，结果，三者相辅相成，浑然一体，避免重复。

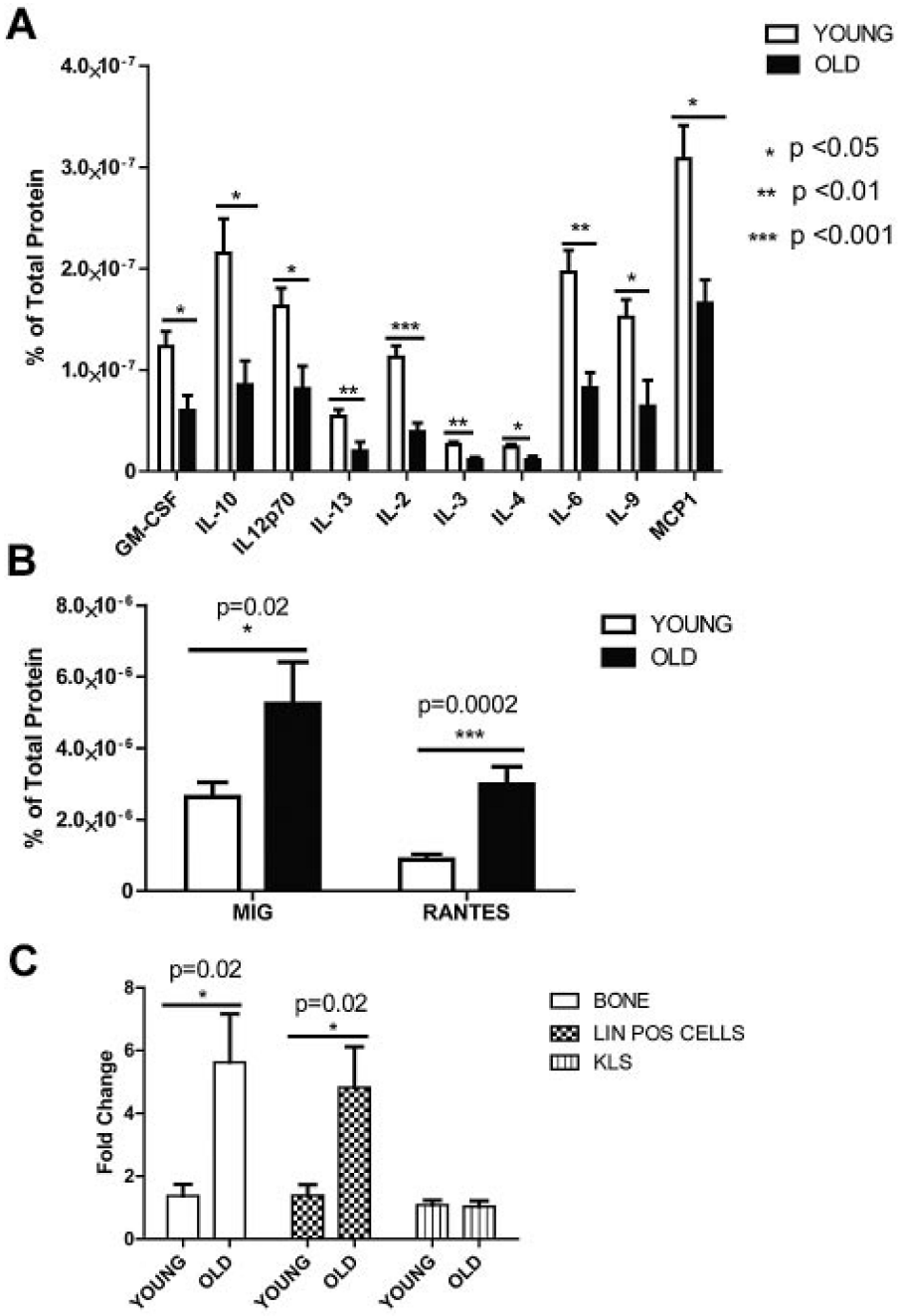

Figure 2. Cytometric bead array on aged and young BM and real-time PCR analysis for Rantes expression in old and young BM populations.

Cytokine levels in the BM were detected with a mouse cytokine bead array and FacsArray plate reader (both from BD Biosciences). We purchased each cytokine's cytometric bead array kit from BD Biosciences which can detect picogram levels of protein in serum or cell-culture supernatant (Flex set; BD Biosciences) and used in a multiplex manner.

(A) Graph represents protein levels of cytokines either in the old or young BM supernatant normalized to total protein levels.

(B) Graph represents Mig and Rantes protein levels either in the old or young BM supernatant (n 10 young, n 6 old).

(C) Quantitave real-time PCR analysis of Rantes on mRNApurified from old or young bone cells, lineage-positive and hematopoietic stem-progenitor (KLS) cells (n 3 young, n 3 old). Error bars represent SEM.

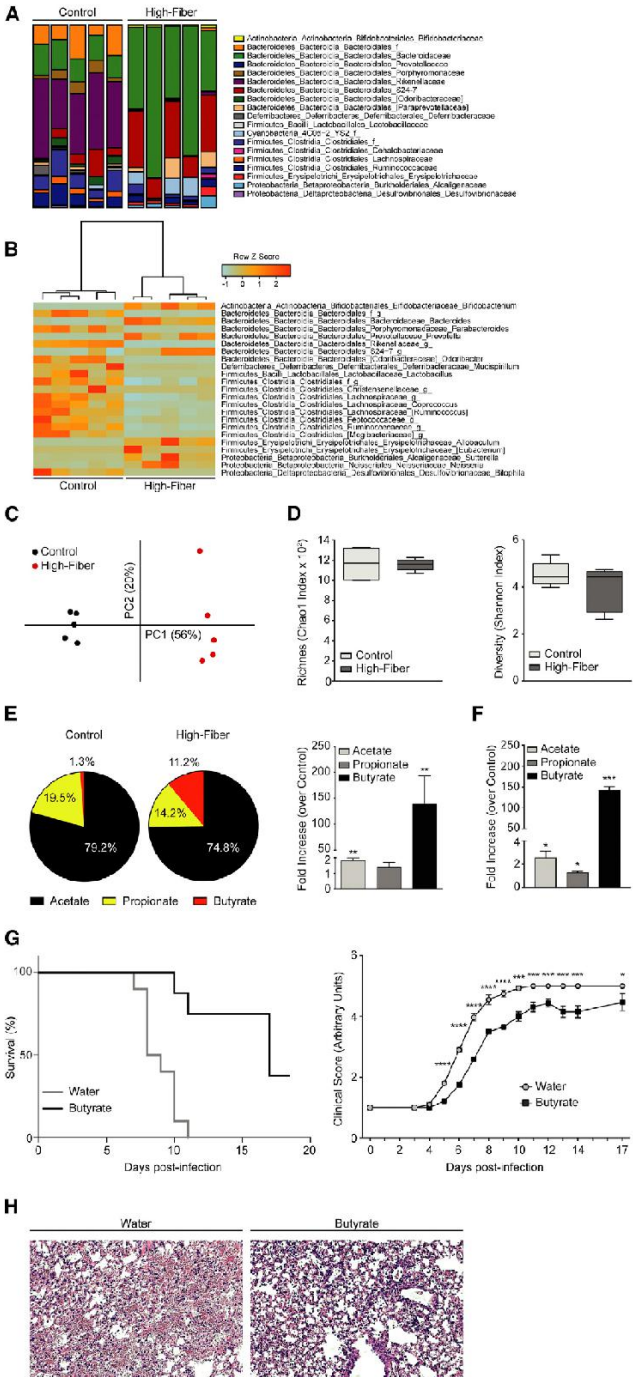

Figure 2. Dietary Fiber Protects against Influenza-Induced Pathology by Altering Gut Microbial Composition and Short-Chain Fatty Acid (SCFA) Levels

(A) Stacked bar plots showing the relative abundance of bacterial operational taxonomic units (OTUs) at family level for each individual of naive control or HFD-fed mice.

(B) Heatmap displaying main OTUs with significant differences in relative abundance among experimental groups with color-code representing row-scaled z-scores.

(C) Principal coordinates analysis (PCoA) based on Bray-Curtis dissimilarity matrix among all samples (ANOSIM $R^2 = 0.27$, $p = 0.00794$).

(D) Taxa richness (Chao1 index) and diversity (Shannon index) boxplots showing the median with min to max values.

(E) Composition of the three main SCFAs (acetate, propionate, and butyrate) in the feces of control and HFD-fed mice and their fold-increase over the control group in dry weight.

(F) Fold-increase of the three main SCFAs (acetate, propionate, and butyrate) in the serum of HFD-fed mice in comparison to the control group.

(G) Survival ($p = 0.0002$) and clinical score of mice treated with butyrate during the course of high-dose infection.

(H) Representative H&E-stained lung tissue from control mice or mice receiving butyrate in drinking water on day 7 after high-dose infection. Scale bars, 100 μm.

Results are representative of data generated in three independent experiments and are expressed as mean ± SEM; n = 3–6 per group in (A)–(F); n = 8–10 per group in (G) and (H). Statistical significance was determined with Mantel-Cox test for the survival in (G) and with Student's t test (unpaired, two-tailed) in (E)–(G). *$p = 0.05$, **$p = 0.01$, ***$p = 0.001$, ****$p = 0.0001$.

Graphical Abstract

- 直观表现研究主题和结果；
- 宣传需要；
- 研究工作过程中多留意；
- 国自然标书申请的加分项（不要低估“颜控”reviewer比例）。

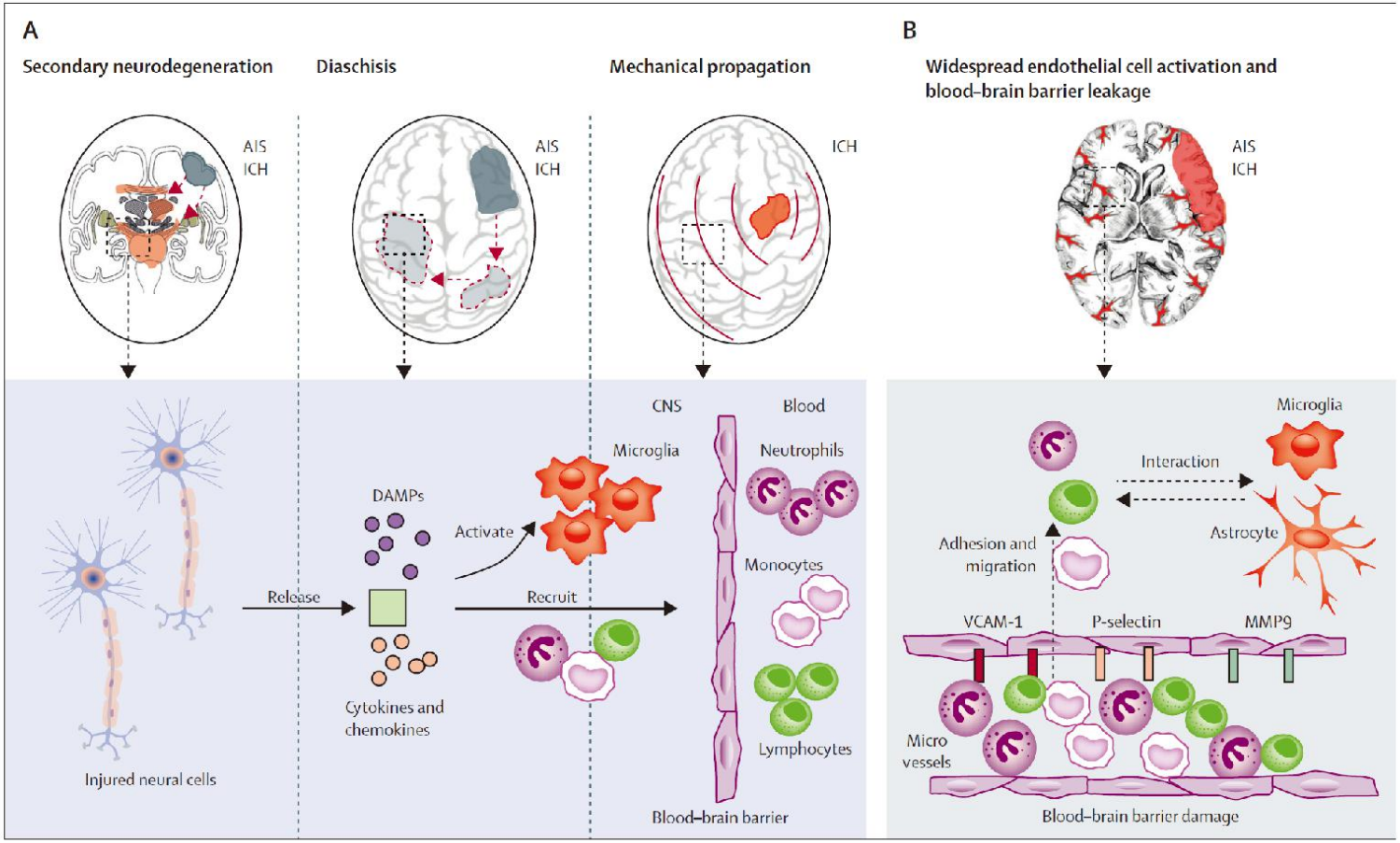

图不是重点；**“箭头”**是关键；平时多留意，用时有准备

当你没有想法时，多读文章

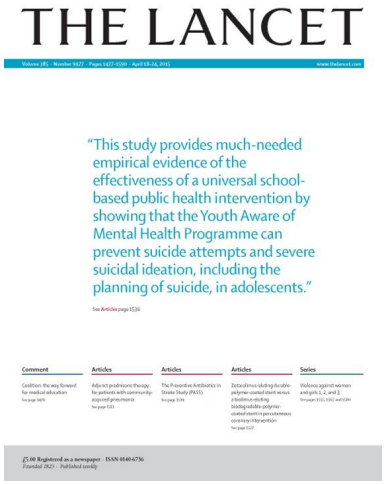

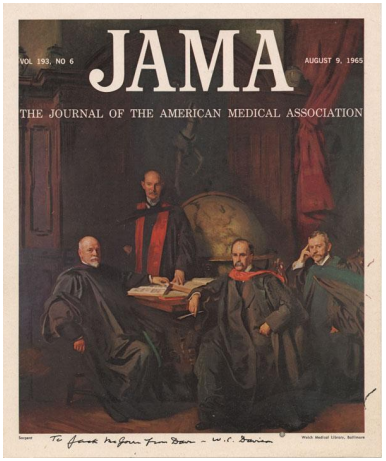

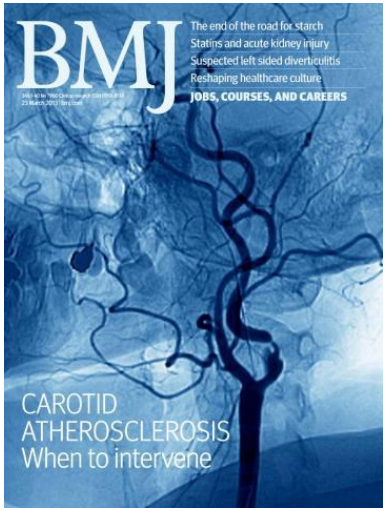

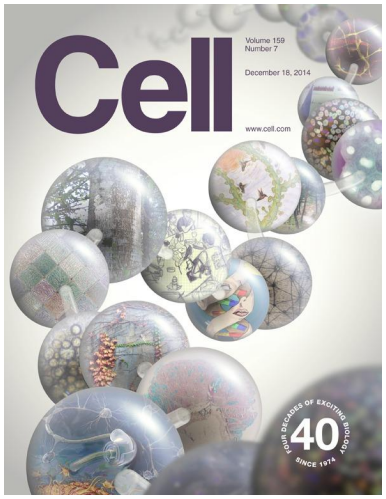

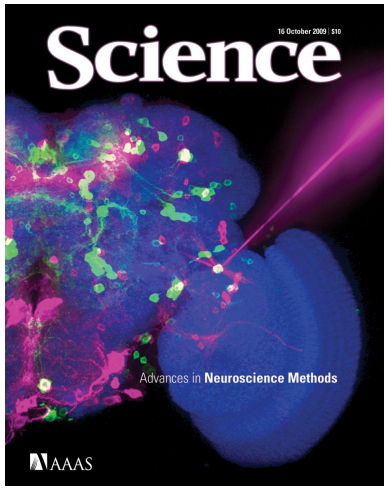

Mimic

Surpass

Create

The World of Science

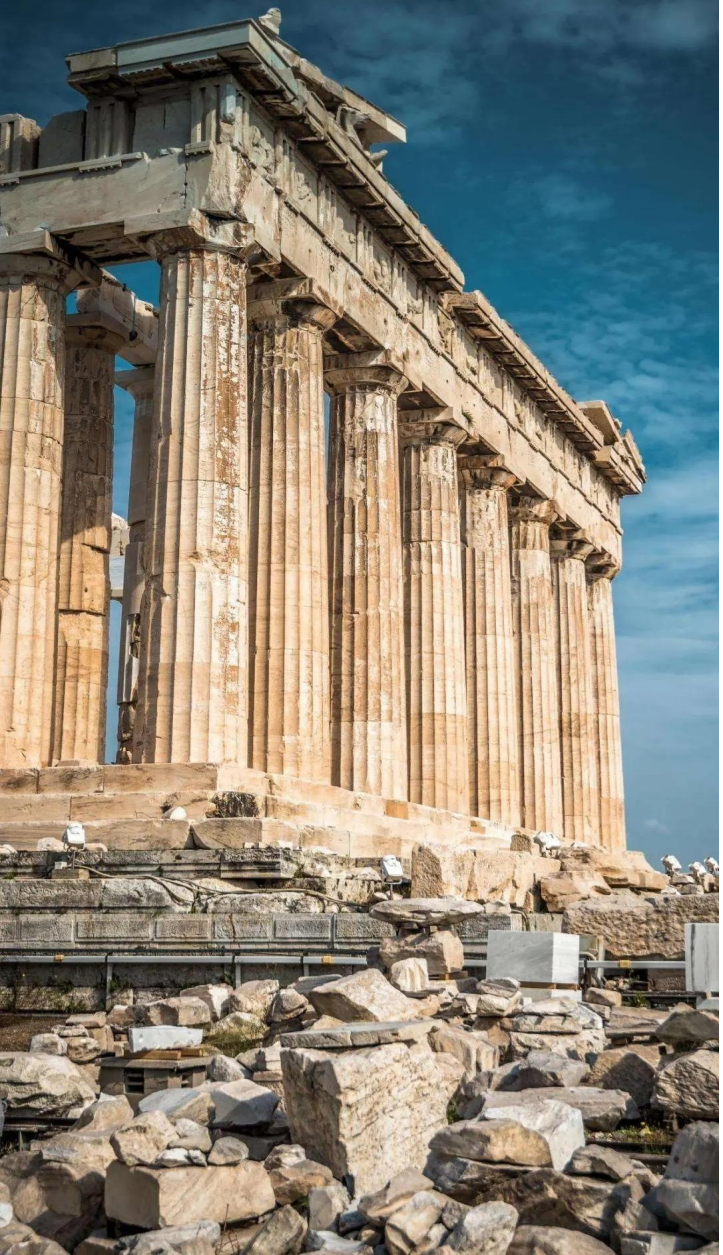

Classic vs Contemporary

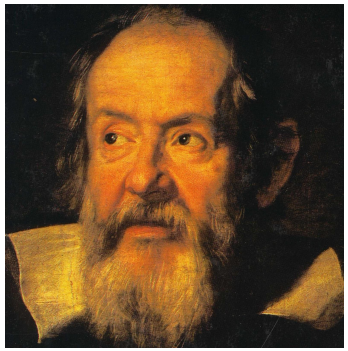

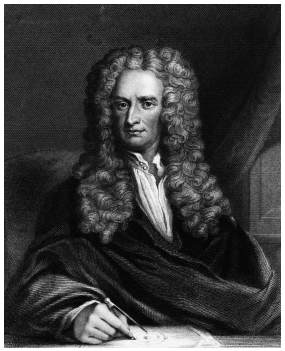

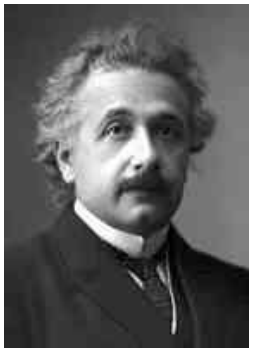

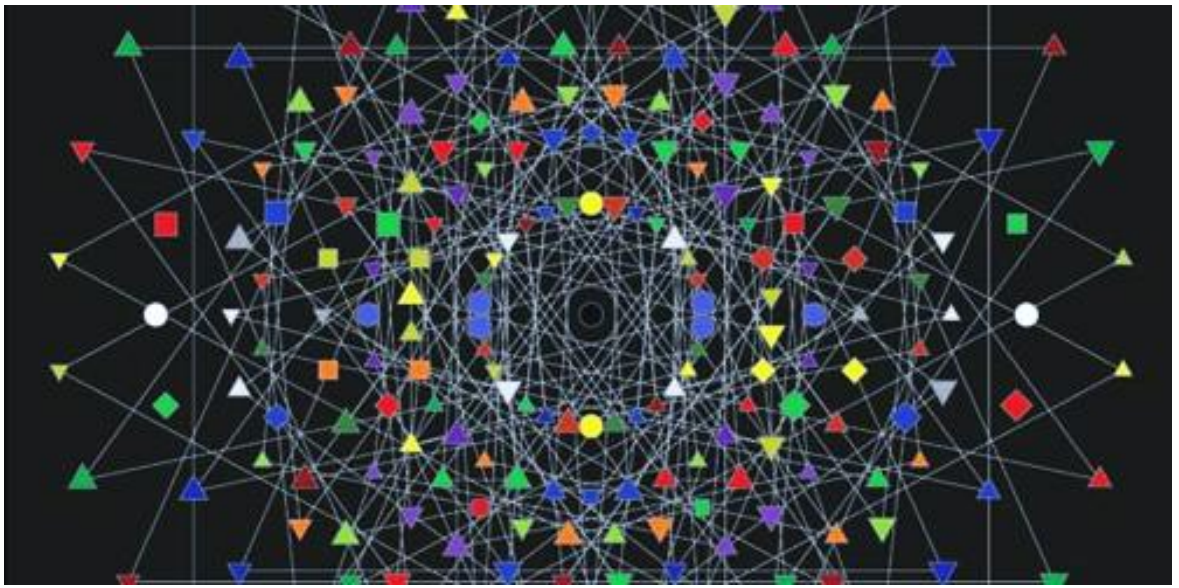

Research needs training


仔细观察世界，小心谨慎地描述